Avery Final Report: Identification and Cross-Directional Control of Coating Processes

Richard D. Braatz, Matthew L. Tyler, and Manfred Morari
Chemical Engineering, 210-41
California Institute of Technology
Pasadena, CA 91125
(818)356-4576 and (818)356-4186

Control and Dynamical Systems (CDS) Technical Report
August 31, 1991

Abstract

Coating refers to the covering of a solid with a uniform layer of liquid. Of special industrial interest is the cross-directional control of coating processes, where the cross-direction refers to the direction perpendicular to the substrate movement. The objective of the controller is to maintain a uniform coating under unmeasured process disturbances.

Assumptions that are relevant to coating processes found in industry are used to develop a model for control design. We show how to identify the model from input-output data. This model is used to derive a model predictive controller to maintain flat profiles of coating across the substrate by varying the liquid flows along the cross direction.

The model predictive controller computes the control action which minimizes the predicted deviation in cross-directional uniformity. The predictor combines the estimate obtained from the model with the measurement of the cross-directional uniformity to obtain a prediction for the next time step. A filter is used to obtain robustness to model error and insensitivity to measurement noise. The tuning of the noise filter and different methods for handling actuator constraints are studied in detail. The three different constraint-handling methods studied are: the weighting of actuator movements in the objective function, explicitly adding constraints to the control algorithm, *i.e.* constrained model predictive control, and scaling infeasible control actions calculated from an unconstrained control law to be feasible.

Actuator constraints, measurement noise, model uncertainty, and the plant condition number are investigated to determine which of these limit the achievable closed loop performance. From knowledge of how these limitations affect the performance we find how the plant could be modified to improve the process uniformity. Also, because identification of model parameters is time-consuming and costly, we study how accurate the identification must be to achieve a given level of performance.

The theory developed throughout the paper is rigorously verified though simulations and experiments on a pilot plant. The effect of interactions on the closed loop performance is shown to be negligible *for this pilot plant.* The measurement noise and the actuator constraints are shown to have the largest effect on closed loop performance.

Contents

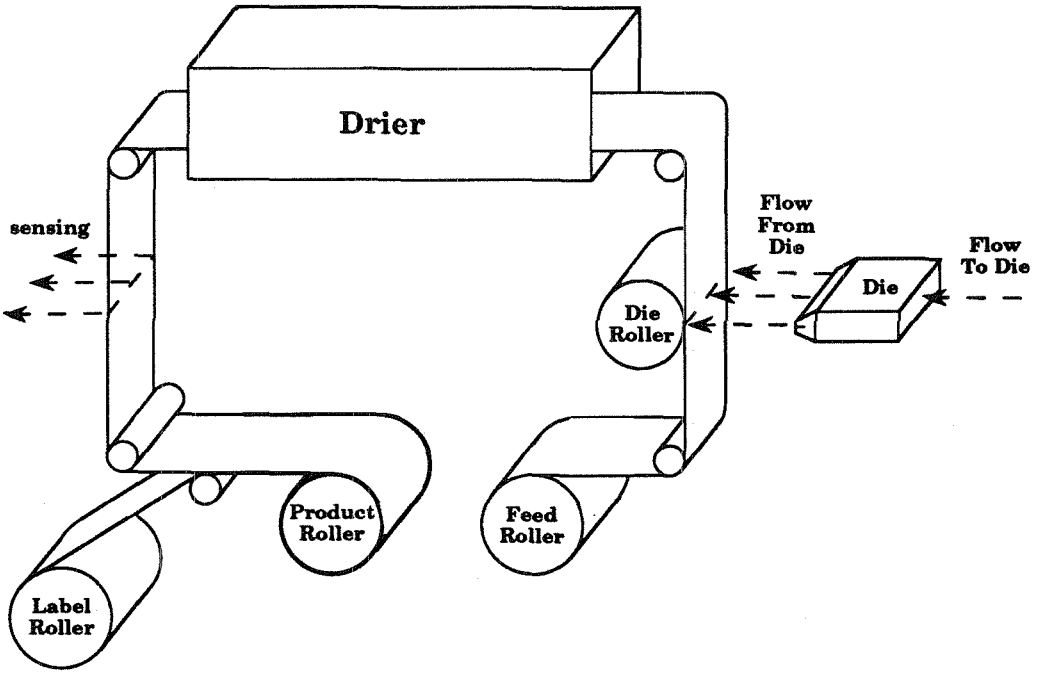

Figure 1: Typical Label-Producing Plant

1 Introduction

Adhesive coating refers to the coating of paper with a uniform layer of adhesive. An example of a process which requires adhesive coating is the production of labels.

Description of a Plant That Produces Labels Fig. 1 is a simplified diagram of a typical plant that produces labels. The process begins with a feed roller from which silicon-coated paper is unwound. From there, the paper passes between a roller and a stainless steel die. The adhesive flows through a slot in the die to the silicon-coated side of the paper. The cavity in the die is designed to distribute a uniform flow of adhesive through the slot. A controlled pump supplies a constant flow of adhesive through the die.

The term "gap width" refers to the distance across the slot at a given point along the die. The gap widths are difficult to measure directly while the die is in use, so strain gauges are calibrated to gap widths when the die is not in use, and used to approximate the gap widths when the die is in use. The gaps through which adhesive flows are adjusted by means of n equally spaced bolts. The bolts are turned manually.

After being coated with adhesive, the paper passes through a drier. After the drier, the time-averaged adhesive thickness at each of the n positions corresponding to the die bolts is measured by an infrared sensor. A layer of paper from the label roller is laminated to the adhesive-coated paper and wound on the product roller. The paper on the product roller is taken elsewhere to be cut and printed to make labels. The paper from the label roller adheres to the adhesive and forms the sticky part of the label. The silicon-coated paper is the backing of the label that is discarded when the sticky part of the label is removed.

The Control Objective The cross-directional control problem is aimed at the maintenance of a uniform profile of adhesive across the paper. Successful control of adhesive thickness improves product quality and reduces the time needed to bring the plant on-line. Poor control can lead not only to adhesive thickness nonuniformity but also coating instabilities that leave portions of the paper uncovered; such paper must be rejected (for a short summary of coating instabilities, see [6]).

We will consider coating processes with a large time delay between a change in gap width and the resulting sensing of the change in coating profile downstream. This time delay could be due to a slow sensor as in the label-producing plant considered above, or due to manual adjustment of the gap widths. The controller cannot be expected to reject disturbances faster than this time delay, so detailed process dynamics are not considered in the modeling, identification, and control of the cross-directional coating process. Thus the objective of the controller is the elimination of slow disturbances in the coating thickness. The disturbances were of this nature in the Avery pilot plant; the control of this plant is studied in Section 6.

Organization Assumptions that are relevant to a subset of adhesive coating processes found in industry are used to develop a model for control design. This model is used to derive an unconstrained model predictive controller to maintain flat profiles of adhesive across the paper by varying the gap widths. Several modifications to the unconstrained controller are proposed to prevent physically infeasible actuator movements (gap widths). The simplest yet effective constraint-handling method is chosen, and the resulting control algorithm is presented in a form for convenient computer implementation.

Actuator constraints, measurement noise, model uncertainty, and the plant condition number are investigated to determine which of these limit the achievable closed loop performance. The theory developed throughout the paper is rigorously verified though simulations and experiments on a pilot plant adhesive coating process at the Avery Research Center in Pasadena.

Notation All scalars are italicized. Matrices are upper case bold. $M_{i,j}$ represents the (i,j) element of the matrix $\mathbf{M}$. Vectors are lower case and bold. The ith element of the vector $\mathbf{x}$ is represented as x_i. $\mathbf{x}(t)$ refers to the value for $\mathbf{x}$ at time t.

2 Model Development

We assume that the control task is carried out by a computer. The controlled output signal $\breve{\mathbf{x}}$ is sampled at intervals T_s resulting in a sequence of measurements $\{\breve{\mathbf{x}}(0), \breve{\mathbf{x}}(1), \ldots, \breve{\mathbf{x}}(h), \ldots\}$ where the arguments $0, 1, \ldots, h, \ldots$ denote time measured in multiples of the sampling interval T_s. On the basis of this sequence the control algorithm determines a sequence of inputs $\{\breve{\mathbf{u}}(0), \breve{\mathbf{u}}(1), \ldots, \breve{\mathbf{u}}(h), \ldots\}$. The input time function $\breve{\mathbf{u}}$ is obtained by holding the input constant over a sampling interval:

$$\breve{\mathbf{u}}(t) = \breve{\mathbf{u}}(h) \qquad hT_s < t \leq (h+1)T_s. \tag{1}$$

The appropriate control action depends on the behavior of the plant to changes in its inputs $\breve{\mathbf{u}}$. The control algorithm is designed based on a *model* for the plant which approximately describes the plant's input-output behavior. We are looking for a model which allows us to determine the sequence of outputs $\{\breve{\mathbf{x}}(0), \breve{\mathbf{x}}(1), \ldots, \breve{\mathbf{x}}(h), \ldots\}$ resulting from a sequence of inputs $\{\breve{\mathbf{u}}(0), \breve{\mathbf{u}}(1), \ldots, \breve{\mathbf{u}}(h), \ldots\}$.

We are not only interested in the response of the plant to the manipulated variables $\breve{\mathbf{u}}$ but also in its response to other inputs, for example, a disturbance $\breve{\mathbf{d}}$. We will use the symbol $\breve{\mathbf{v}}$ to denote any inputs other then the control inputs $\breve{\mathbf{u}}$. These inputs will also be represented as a sequence $\{\breve{\mathbf{v}}(0), \breve{\mathbf{v}}(1), \ldots, \breve{\mathbf{v}}(h), \ldots\}$.

Below we make assumptions on the plant that are relevant to a subset of adhesive coating processes found in industry. These assumptions are used to develop a dimensional model. This model is transformed to a dimensionless form. We show how to determine the dimensionless model parameters theoretically or from experimental input-output data. The dimensionless model is then rearranged into a form suitable for controller design.

2.1 Dimensional Model

Consider a plant with the number of actuators n equal to the number of sensors (or sensor measurement positions). It can be shown theoretically and experimentally (through examination of pilot plant data) that the plant approximately behaves linearly in the operating region. Let $\breve{\mathbf{u}}$ be the vector of gap widths, $\breve{\mathbf{x}}$ be the vector of adhesive thicknesses, and $\breve{\mathbf{v}}$ collect any effects on the adhesive thicknesses not due to changes in gap widths. Then the adhesive thicknesses at sampling instant t is related to the gap widths at the previous sampling instant through

$$\breve{\mathbf{x}}(t) = \mathbf{P}\breve{\mathbf{u}}(t-1) + \breve{\mathbf{v}}(t), \tag{2}$$

where $\mathbf{P}$ is a constant $n \times n$ matrix.

Assumption on $\breve{\mathbf{v}}$ $\breve{\mathbf{v}}$ accounts for unmeasured input effects such as measurement noise and disturbances. Assumptions on $\breve{\mathbf{v}}$ will be important for tuning of the noise filter introduced in Section 3.1. Assume that $\breve{\mathbf{v}}$ is non-zero-mean stochastic variable, *i.e.* $\{\breve{\mathbf{v}}(0), \breve{\mathbf{v}}(1), \ldots, \breve{\mathbf{v}}(h), \ldots\}$ is a sequence of independent random vectors with non-zero mean (for example, see [4]). Define the steady-state disturbance $\breve{\mathbf{d}}$ as the time-averaged value of $\breve{\mathbf{v}}$, and define $\breve{\mathbf{n}}$ by

$$\breve{\mathbf{n}}(t) = \breve{\mathbf{v}}(t) - \breve{\mathbf{d}}. \tag{3}$$

Then $\breve{\mathbf{n}}$ is white noise and will be referred to as the measurement noise.

$\breve{\mathbf{v}}$ is assumed to be non-zero-mean stochastic variable. This description worked well for the Avery pilot plant discussed in Section 6, and is expected in general to be a good assumption. Though the die was designed to give a uniform coating thickness when the gap widths are equal, this was not true in practice. In practice equal gap widths do not give a uniform coating because of imperfections in the roller or the die, non-uniformities in the drying process, or poor calibration of the gap widths. These imperfections lead $\breve{\mathbf{v}}$ to have non-zero mean. $\breve{\mathbf{v}}$ was chosen to be stochastic because this described well the apparently random fluctuations of the process, and especially the random fluctuations in the infrared sensor.

Assumptions on P Typically, the total flow of adhesive through the die is maintained constant through a high gain controller. Because of constant total flow, increasing the flow through one actuator will necessitate decreasing the flow through the others. In the development of the model, we make the following assumptions:

1. The total adhesive flow (and the sum of the adhesive coating thicknesses) is constant.
2. All actuators and sensors are equivalent.
3. The only interactions between actuators are due to the constant flow assumption.
4. An increase in one gap width results in a uniform decrease in the flow through all gaps.

Assumption 2 implies that $\mathbf{P}$ is symmetric. Assumption 3 implies that $\mathbf{P}$ can be separated into two matrices

$$\mathbf{P} = \breve{k}\mathbf{I} - \mathbf{M}, \tag{4}$$

where $\breve{k}$ is the gain between the ith gap width and its corresponding adhesive thickness for an infinitely wide die (*i.e.* $n \to \infty$), $\mathbf{I}$ is the $n \times n$ identity matrix, $\breve{k}\mathbf{I}$ is the contribution that changing gap widths would have on the adhesive thicknesses if there were no interactions, and $\mathbf{M}$ represents the effect that increasing one gap width has on decreasing the flow through all the gaps. Assumption 4 implies that all elements of $\mathbf{M}$ are equal, *i.e.* $M_{i,j} = \nu$ for $i, j = 1, 2, \cdots, n$. Then

$$\mathbf{P} = \underbrace{\begin{pmatrix} \breve{k}-\nu & -\nu & -\nu & \cdots & -\nu \\ -\nu & \breve{k}-\nu & -\nu & \ddots & \vdots \\ -\nu & \ddots & \ddots & \ddots & -\nu \\ \vdots & \ddots & \ddots & \breve{k}-\nu & -\nu \\ -\nu & \cdots & -\nu & -\nu & \breve{k}-\nu \end{pmatrix}}_{n \times n}. \tag{5}$$

Assumption 1 is that $\sum_{i=1}^{n} \breve{x}_i$ is a constant for all gap widths $\breve{\mathbf{u}}$. Then (ignoring noise $\breve{\mathbf{n}}$), we have from (2) that

$$\sum_{i=1}^{n} \breve{x}_i(t) = \sum_{i=1}^{n} \left(\breve{d}_i + \sum_{j=1}^{n} P_{i,j} \breve{u}_j(t-1) \right) = \sum_{i=1}^{n} \breve{d}_i + \sum_{j=1}^{n} \left(\sum_{i=1}^{n} P_{i,j} \right) \breve{u}_j(t-1) \tag{6}$$

must be a constant for all $\breve{u}_j(t-1)$. This implies that

$$\sum_{i=1}^{n} P_{i,j} = 0, \qquad \text{for } j = 1, 2, \cdots, n. \tag{7}$$

By substituting the elements of $\mathbf{P}$ from (5) into the summation (7), we find that ν must be related to $\breve{k}$ by

$$\nu = \frac{\breve{k}}{n}. \tag{8}$$

Substituting for ν in (5) gives the final form for $\mathbf{P}$:

$$\mathbf{P} = \frac{\breve{k}}{n}\mathbf{B}, \tag{9}$$

where

$$\mathbf{B} = \underbrace{\begin{pmatrix} n-1 & -1 & -1 & \cdots & -1 \\ -1 & n-1 & -1 & \ddots & \vdots \\ -1 & \ddots & \ddots & \ddots & -1 \\ \vdots & \ddots & \ddots & n-1 & -1 \\ -1 & \cdots & -1 & -1 & n-1 \end{pmatrix}}_{n \times n}. \tag{10}$$

The one parameter $\breve{k}$ in the model does not depend on the number of actuators n.

2.2 Dimensionless Model

The model is transformed to a dimensionless form for two reasons. First, using a dimensionless model will allow the control parameters to vary little between different plants. Second, the controller is designed to produce a coating of uniform thickness and will *not* be able to change the mean coating thickness. A flow controller which maintains constant flow to the coating die is used to adjust the mean coating thickness. The non-dimensional variable $\mathbf{x}$ is therefore chosen to represent coating thickness as a deviation from the mean.

Define $\bar{x} = \frac{1}{n}\sum_{i=1}^{n} \breve{x}_i$ and $\bar{u}$ as the nominal gap width. The nominal gap width should be chosen well within the stable coating region. Define the following dimensionless variables:

$$x_i = \frac{\breve{x}_i - \bar{x}}{\bar{x}} \qquad u_i = \frac{\breve{u}_i - \bar{u}}{\bar{u}} \qquad d_i = \frac{\breve{d}_i - \bar{x}}{\bar{x}} \qquad n_i = \frac{\breve{n}_i}{\bar{x}} \qquad k = \frac{\breve{k}\bar{u}}{n\bar{x}}, \tag{11}$$

Solve the above expressions for $\breve{x}_i$, $\breve{u}_i$, $\breve{d}_i$, $\breve{n}_i$, and $\breve{k}$, substitute into (2), and rearrange to give the dimensionless model:

$$\mathbf{x}(t) = k\mathbf{B}\mathbf{u}(t-1) + \mathbf{d} + \mathbf{n}(t). \tag{12}$$

2.3 Determination of the Dimensionless Gain k

We show how to determine the gain theoretically (off-line) or from experimental input-output data (on-line).

2.3.1 Off-Line Determination

We show how to determine the dimensional gain $\breve{k}$ off-line. The dimensionless gain is then found from (11).

For an example, consider the label-producing plant described in the introduction. The overall gain $\breve{k}$ is the product of the gains for the individual process components, *i.e.*

$$\breve{k} = \breve{k}_{\mathrm{s}} \cdot \breve{k}_{\mathrm{d}} \cdot \breve{k}_{\mathrm{a}}, \tag{13}$$

where $\breve{k}_{\mathrm{s}}$, $\breve{k}_{\mathrm{d}}$, and $\breve{k}_{\mathrm{a}}$ are gains for the sensor, the drier, and the actuator respectively.

The gain for the sensor $\breve{k}_{\mathrm{s}}$ is easy to measure off-line. It is calibrated to measure the thickness of the organics on the substrate. The drier does not change the amount of organics on the substrate, so the gain for the drying process $\breve{k}_{\mathrm{d}}$ is unity.

The gain for the actuator is the product of the gain between true gap widths to adhesive thicknesses, and the gain for the strain gauges. The gain for the strain gauges can be calculated from the geometry of the metal and knowledge of the metal's physical properties, but it is easier to calibrate the strain gauges off-line.

The adhesive thicknesses can be calculated from mass and momentum conservation and a finite element method. The finite element method requires the viscosity to shear relationship for the adhesive, the internal geometry of the die, and boundary conditions between the adhesive and the die, between the adhesive and the paper on the roller, and between the adhesive and the air [6]. The gain between the true gap widths to adhesive thicknesses can then be found by perturbing the gap widths and numerically calculating the change in adhesive thicknesses.

The dimensionless gain k is calculated from the dimensional gain $\breve{k}$ using (11). Considering the amount of effort required to determine k off-line through accurate modeling of the process components, it may be simpler to measure k experimentally.

2.3.2 On-Line Identification

We now consider the identification of k from input-output data. Various changes are made in the inputs (gap widths), and the resulting adhesive thicknesses are measured. Let m represent the number of open loop experiments, *i.e.* input-output pairs. Use (11) to convert all inputs and outputs to dimensionless form. A superscript ^{i} refers to the ith experment, so $\mathbf{u}^i$ refers to the input of the ith experiment, $\mathbf{x}^i$ refers to the output of the ith experiment, and $\mathbf{v}^i$ refers to the effect of the unmeasured inputs. The inputs $\mathbf{u}^i$ should be chosen as large as possible to diminish the effect of the unmeasured inputs. The standard parameter fitting algorithm employed in identification is the least squares algorithm.

Write (12) for each experiment where the time argument is suppressed to simplify the notation ($\mathbf{v}^i = \mathbf{d}^i + \mathbf{n}^i$)

$$\mathbf{x}^i = k\mathbf{B}\mathbf{u}^i + \mathbf{v}^i \qquad\qquad i = 1, \ldots, m. \tag{14}$$

Stack these equations on top of each other and rearrange to give

$$\begin{pmatrix} \mathbf{x}^1 \\ \vdots \\ \mathbf{x}^m \end{pmatrix} - \begin{pmatrix} \mathbf{B}\mathbf{u}^1 \\ \vdots \\ \mathbf{B}\mathbf{u}^m \end{pmatrix} k = \begin{pmatrix} \mathbf{v}^1 \\ \vdots \\ \mathbf{v}^m \end{pmatrix}. \tag{15}$$

Define

$$\mathbf{a} = \begin{pmatrix} \mathbf{B}\mathbf{u}^1 \\ \vdots \\ \mathbf{B}\mathbf{u}^m \end{pmatrix}, \qquad \mathbf{b} = \begin{pmatrix} \mathbf{x}^1 \\ \vdots \\ \mathbf{x}^m \end{pmatrix}, \qquad y = k, \qquad \text{and} \qquad \mathbf{z} = -\begin{pmatrix} \mathbf{v}^1 \\ \vdots \\ \mathbf{v}^m \end{pmatrix}. \tag{16}$$

We are interested in fitting the dimensionless plant gain k. Assume that the unmeasured variables $\mathbf{v}^i$ are independent of the inputs $\mathbf{u}^i$. Then a natural objective for selecting k is to minimize the square norm of the residual vector $\mathbf{z} = \mathbf{a}y - \mathbf{b}$. This is the least squares problem

$$\min_y (\mathbf{a}y - \mathbf{b})^T(\mathbf{a}y - \mathbf{b}). \tag{17}$$

The solution $y = k$ that solves the least squares problem is given by

$$k = y = (\mathbf{a}^T\mathbf{a})^{-1}\mathbf{a}^T\mathbf{b}. \tag{18}$$

2.4 Model for Control Design

Augmenting the Model $\mathbf{B}$ in (10) is singular. This is because the coating thicknesses $\mathbf{x}$ are not uniquely determined by the gap widths $\mathbf{u}$. Any increment in gap width added to all the gap widths u_i does not change the coating thicknesses. However, to keep a stable film, the dimensionless gap widths $\mathbf{u}$ must not stray too far from the preferred position of $\mathbf{0}$. We augment the model with the additional equation $\sum_{i=1}^{n} u_i = 0$ to both keep $\mathbf{u}$ from straying and to give a unique mapping of the coating thicknesses to the gap widths. This is done as follows:

- Add a component to $\mathbf{x}$, $\mathbf{d}$, and $\mathbf{n}$, and set this component to zero, *i.e.* $x_{n+1} = n_{n+1} = d_{n+1} = 0$.
- Add a row of ones to the plant matrix $k\mathbf{B}$ to give the new $n+1$ by n plant matrix $\mathbf{C} = \begin{bmatrix} k\mathbf{B} \\ 1 \cdots 1 \end{bmatrix}$.

This leads to the augmented model

$$\mathbf{x}(t) = \mathbf{C}\mathbf{u}(t-1) + \mathbf{d} + \mathbf{n}(t). \tag{19}$$

Since the mean value of $\mathbf{u}$ is a *free* degree of freedom (it does not change coating thicknesses), a controller design based on the above model which seeks to minimize $\mathbf{x}$ will automatically adjust its control action so that the mean value of $\mathbf{u}$ will be exactly zero. Also, the singularity of the original gain matrix $\mathbf{B}$ is removed.

Model in terms of $\Delta\mathbf{u}(t-1)$ To derive the model predictive controller in the next section, it is convenient to express the model in terms of the changes in the inputs rather than the inputs themselves. For this purpose, we subtract the equation (19) for $t-1$ from that at t to arrive at

$$\mathbf{x}(t) = \mathbf{x}(t-1) + \mathbf{C}\Delta\mathbf{u}(t-1) + \Delta\mathbf{n}(t), \tag{20}$$

where

$$\Delta\mathbf{u}(t-1) = \mathbf{u}(t-1) - \mathbf{u}(t-2) \tag{21}$$

$$\Delta\mathbf{n}(t) = \mathbf{n}(t) - \mathbf{n}(t-1) \tag{22}$$

$$\tag{23}$$

The controller will calculate the inputs to the plants based on measured variables. The model for control design is:

$$\mathbf{x}(t) = \mathbf{x}(t-1) + \mathbf{C}\Delta\mathbf{u}(t-1), \tag{24}$$

3 Estimation and Prediction

Recall that our objective for using a model is to predict the effect of changes in gap widths on the adhesive thicknesses. This will allow us to find the "best" adjustments in gap widths to reject disturbances.

3.1 State Estimation - Filter

Note from (24) that $\mathbf{x}(t)$ is the model prediction of the adhesive thickness at time t and should ideally equal $\hat{\mathbf{x}}(t)$, the measured dimensionless adhesive thickness at time t. However, we do not expect our model (24) to perfectly describe the system and could therefore observe an undesirable offset between $\hat{\mathbf{x}}(t)$ and $\mathbf{x}(t)$ for large t. Let us introduce the notation $\mathbf{x}(\cdot|t-1)$ to denote the estimate of $\mathbf{x}(\cdot)$ obtained from all available measurement information up to $t-1$. With this notation, the analogous form of equation (24) is given by:

Model Prediction:

$$\mathbf{x}(t|t-1) = \mathbf{x}(t-1|t-1) + \mathbf{C}\Delta\mathbf{u}(t-1). \tag{25}$$

Because we do not expect our model to perfectly describe the system, we correct the model prediction $\mathbf{x}(t|t-1)$ based on the difference between the measurement $\hat{\mathbf{x}}(t)$ at time t and the model prediction for this time step.

Correction:

$$\mathbf{x}(t|t) = \mathbf{x}(t|t-1) + \gamma\left[\hat{\mathbf{x}}(t) - \mathbf{x}(t|t-1)\right], \qquad \gamma \in (0,1]. \tag{26}$$

It would be justifiable to add the total difference between the measurement $\hat{\mathbf{x}}(t)$ and the model prediction $\mathbf{x}(t|t-1)$ if the difference were solely due to a constant disturbance effect. If the difference were solely due to measurement noise, then we would not want to correct the model prediction at all. In general, disturbances, model error, and measurement noise will contribute to the difference, in which case a more cautious approach than adding the total difference will be appropriate. This is achieved by filtering the correction term with $\gamma \in (0,1]$.

Thus rather than correct the model prediction by the full error $[\hat{\mathbf{x}}(t) - \mathbf{x}(t|t-1)]$, one takes a more cautious approach and utilizes only a fraction γ. The larger the measurement noise, the smaller γ should be chosen.

By substituting (25) into (26) we obtain the *state estimator*

$$\mathbf{x}(t|t) = (1-\gamma)\left[\mathbf{x}(t-1|t-1) + \mathbf{C}\Delta\mathbf{u}(t-1)\right] + \gamma\hat{\mathbf{x}}(t), \tag{27}$$

which allows one to compute the current state estimate $\mathbf{x}(t|t)$ based on the previous estimate $\mathbf{x}(t-1|t-1)$, the previous input move $\Delta\mathbf{u}(t-1)$, and the current measurement $\hat{\mathbf{x}}(t)$.

The state estimator (27) suggests that $\mathbf{x}(t|t)$ is a filtered version of $\hat{\mathbf{x}}$. Indeed, in a noise-free system with the manipulated variables constant, we have

$$\mathbf{x}(t|t) = (1-\gamma)\mathbf{x}(t-1|t-1) + \gamma\hat{\mathbf{x}}(t), \tag{28}$$

which gives the state estimate $\mathbf{x}(t|t)$ as $\hat{\mathbf{x}}$ passed through a first order filter. If the output $\hat{\mathbf{x}}$ suddenly changes to a constant value then the state estimate $\mathbf{x}(t|t)$ approaches the true value $\hat{\mathbf{x}}$ with the filter time constant:

$$\tau = \frac{\mathrm{T_s}}{\log\left(\frac{1}{1-\gamma}\right)}, \tag{29}$$

where T_s is the time between sampling instances [3].

3.2 Prediction

The control algorithm prescribes the gap widths $\mathbf{u}$ which reject disturbances in $\mathbf{x}$. In order for the control algorithm to determine the "best" current gap widths there has to be a means of *predicting* the effect of the gap widths on the future adhesive thicknesses $\mathbf{x}$. The predictor is given by writing (25) for the next time step $t+1$:

$$\mathbf{x}(t+1|t) = \mathbf{x}(t|t) + \mathbf{C}\Delta\mathbf{u}(t) \tag{30}$$

4 Control

We begin by stating the unconstrained control objective. Then we derive the unconstrained controller that minimizes this objective. We discuss different methods of modifying this controller to handle actuator constraints, in our case constraints in adjacent gap widths. We choose the simplest yet effective constraint-handling method to use for our control problem, and finish the section with the algorithm to implement on the computer.

4.1 Objective

Performance Criteria The performance criteria (in our case the rejection of slow disturbances) must be expressed in mathematical terms so that the control law can be obtained in algorithmic form. We will choose to minimize the quadratic objective

$$z = \|\mathbf{x}(t+1|t)\|^2, \tag{31}$$

where $\|\cdot\|$ represents the Euclidean norm, $\|x\|^2 = \sum_{i=1}^{n} x_i^2$. This criterion minimizes the sum of the squared deviations of the adhesive thicknesses, which penalizes large deviations proportionally more than smaller ones so that on the average the adhesive thicknesses $\mathbf{x}$ remains close to zero and large excursions are avoided. We chose to weight the deviations equally across the paper.

It is common in model predictive control to include in the objective a weighted norm of the manipulated variables as in

$$z = \|\mathbf{x}(t+1|t)\|^2 + \alpha\|\Delta\mathbf{u}(t)\|^2. \tag{32}$$

This is done to keep the control action from moving too abruptly between consecutive sampling instances. We assume the operator has enough time to make the gap adjustments suggested by the control algorithm, so this extra term is unnecessary.

The Unconstrained Control Problem We express the control problem as an optimization by combining the objective (31) with the predictor (30):

$$\min_{\Delta\mathbf{u}(t)} \|\mathbf{x}(t+1|t)\|^2, \qquad \text{where } \mathbf{x}(t+1|t) = \mathbf{x}(t|t) + \mathbf{C}\Delta\mathbf{u}(t). \tag{33}$$

4.2 Least Squares Solution of the Unconstrained Control Problem

The controller will seek to minimize the predicted non-dimensional coating thickness $\mathbf{x}(t+1|t)$. The control problem is in the form of a least squares problem. To see this, let

$$\mathbf{A} = \mathbf{C}, \quad \mathbf{b} = -\mathbf{x}(t|t), \quad \text{and} \quad \mathbf{y} = \Delta\mathbf{u}(t). \tag{34}$$

Then the control problem (33) is the least squares problem

$$\min_{\mathbf{y}} (\mathbf{A}\mathbf{y} - \mathbf{b})^T (\mathbf{A}\mathbf{y} - \mathbf{b}). \tag{35}$$

The solution $\mathbf{y}$ which minimizes the least square problem is given by

$$\mathbf{y} = (\mathbf{A}^T\mathbf{A})^{-1}\mathbf{A}^T\mathbf{b}. \tag{36}$$

Substituting the appropriate parts of equation (34) into (36) yields the following optimal controller movement:

$$\Delta\mathbf{u}(t) = -(\mathbf{C}^T\mathbf{C})^{-1}\mathbf{C}^T\mathbf{x}(t|t). \tag{37}$$

By substituting equation (21) into (37) we have that the new actuator position $\mathbf{u}(t)$ is calculated from the previous actuator position and the current state estimate $\mathbf{x}(t|t)$:

$$\mathbf{u}(t) = \mathbf{u}(t-1) - (\mathbf{C}^T\mathbf{C})^{-1}\mathbf{C}^T\mathbf{x}(t|t). \tag{38}$$

This is the least-squares optimal controller output. The current state estimate $\mathbf{x}(t|t)$ is calculated from the correction equation (26), and the model prediction $\mathbf{x}(t|t-1)$ in the correction equation (26) is calculated from the model prediction equation (25). The algorithm to implement on the computer will be given Section 4.4.

4.3 Methods of Handling Actuator Constraints

Excessive stresses in the die constrain adjacent actuator positions. We will consider two ways of specifying these constraints. First, the specification could be that the difference between adjacent actuator positions should be limited, *i.e.*

$$|\delta u_i| = |u_{i+1} - u_i| \leq |\delta u|_{max}, \qquad \text{for } i = 1, \ldots, n-1. \tag{39}$$

An additional specification could be that the difference between adjacent actuator positions must be even less when large adjacent gap differences are made in opposite directions. This constraint can be written as

$$|\delta^2 u_i| = |u_{i+2} - 2u_{i+1} + u_i| \leq |\delta^2 u|_{max}, \qquad \text{for } i = 1, \ldots, n-2. \tag{40}$$

For those plants where $|\delta^2 u|_{max} \geq 2|\delta u|_{max}$, the first constraint (39) implies the second constraint (40), so for these plants the second constraint need not be considered.

Constraint-handling will be needed when the disturbances are sufficiently large and have sharp *spatial* variations across the paper. When the disturbances are uniform across the paper, then the control action calculated from the unconstrained control algorithm will be uniform, and constraint-handling is not needed.

Actuator constraints can be handled in three ways: by including additional terms in the objective function, by adding the constraints explicitly to the control algorithm, or by scaling the control actions to be feasible. Below we describe each method of handling actuator constraints. We will choose the simplest yet effective constraint-handling method to use for our control problem.

4.3.1 Additional Terms in the Objective Function

Additional terms weighting $|u_{i+1} - u_i|$ and $|u_{i+2} - 2u_{i+1} + u_i|$ could be added to the objective function (31). The disadvantage of this approach is that the added weighted terms *always* affect the control action. The weights for these terms must be large enough to keep the control action feasible for disturbances which contain sharp spatial variations, but large weights on the control action will substantially slow the control action when the disturbances are uniform across the paper and the extra terms are not needed.

To obtain the control law for this constraint-handling method, first we write the objective function including the additional weighting terms:

$$z = \|\mathbf{x}(t+1|t)\|^2 + \beta_1\|\mathbf{D_1}\mathbf{u}(t)\|^2 + \beta_2\|\mathbf{D_2}\mathbf{u}(t)\|^2, \tag{41}$$

where $\mathbf{D_1}$ and $\mathbf{D_2}$ are linear transformations relating $\mathbf{u}$ to an $(n-1)$-vector and a $(n-2)$-vector representing first and second order differences respectively. These transformations are given by:

$$\mathbf{D_1} = \underbrace{\begin{pmatrix} -1 & 1 & 0 & \cdots & 0 \\ 0 & \ddots & \ddots & \ddots & \vdots \\ \vdots & \ddots & \ddots & \ddots & 0 \\ 0 & \cdots & 0 & -1 & 1 \end{pmatrix}}_{(n-1)\ \times\ n}, \qquad \mathbf{D_2} = \underbrace{\begin{pmatrix} -1 & 2 & -1 & 0 & \cdots & 0 \\ 0 & \ddots & \ddots & \ddots & \ddots & \vdots \\ \vdots & \ddots & \ddots & \ddots & \ddots & 0 \\ 0 & \cdots & 0 & -1 & 2 & -1 \end{pmatrix}}_{(n-2)\ \times\ n}. \tag{42}$$

Using objective function (41) instead of (31) and formulating the resulting control problem as a least square problem similarly as in Section 4.2, the following control algorithm with weighting penalties is obtained:

$$\mathbf{u}(t) = \left[\mathbf{C}^T\mathbf{C} + \beta_1\mathbf{D_1}^T\mathbf{D_1} + \beta_2\mathbf{D_2}^T\mathbf{D_2}\right]^{-1}\mathbf{C}^T\left[\mathbf{C}\mathbf{u}(t-1) - \mathbf{x}(t|t)\right]. \tag{43}$$

In general, there do not exist weighting parameters β_i which result in good performance for a wide range of disturbances. That this is true for the Avery pilot plant is shown through simulations in Section 6.3.1.

4.3.2 Explicitly Adding Constraints to the Control Algorithm

The constraints could be added explicitly to the control algorithm. Then the constrained control problem will be the unconstrained control problem (33) plus the additional constraints (39) and (40):

$$\min_{\Delta\mathbf{u}(t)} \|\mathbf{x}(t+1|t)\|^2, \tag{44}$$

$$\begin{aligned} \text{such that} \quad & \mathbf{x}(t+1|t) = \mathbf{x}(t|t) + \mathbf{C}\Delta\mathbf{u}(t) \\ & |\delta u_i| = |u_{i+1} - u_i| \le |\delta u|_{max}, && \text{for } i = 1,\ldots,n-1. \\ & |\delta^2 u_i| = |u_{i+2} - 2u_{i+1} + u_i| \le |\delta^2 u|_{max}, && \text{for } i = 1,\ldots,n-2. \end{aligned} \tag{45}$$

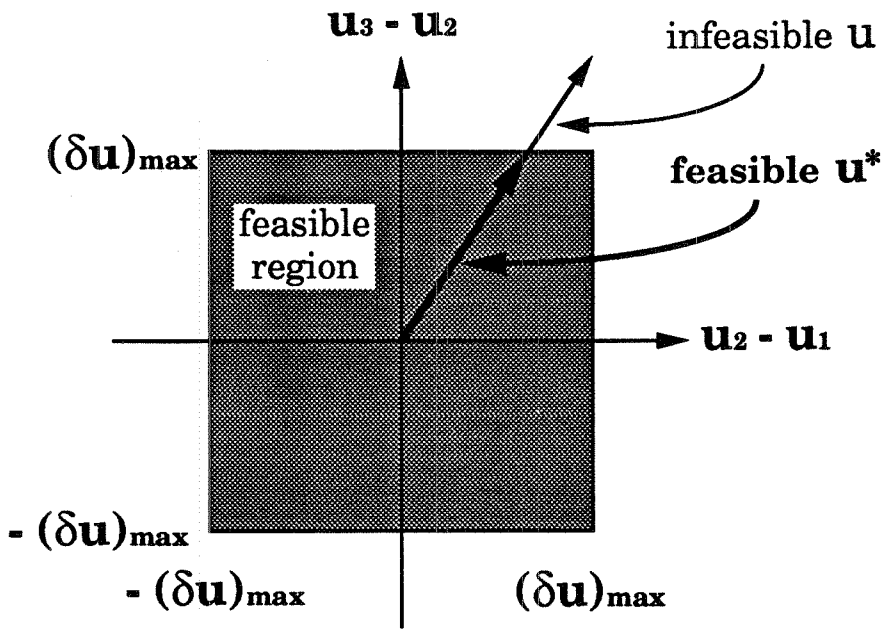

Figure 2: Projection of an infeasible control action to the feasible space.

This is a quadratic programming problem that must be solved at each time step for the optimal actuator movements $\Delta\mathbf{u}(t)$. This approach is not as simple to implement and analyze as the third constraint-handling method discussed next.

4.3.3 Scaling Control Actions

Constraints can be handled by projecting any infeasible $\mathbf{u}$ given by the unconstrained control law (38) to the feasible space. Fig. 2 illustrates this idea for the first constraint (39) for $n = 3$. All feasible control actions $\mathbf{u}$ are given by the shaded region. When the unconstrained control law (38) suggests an infeasible control action, a feasible control action is found by projecting $\mathbf{u}$ to the feasible space. Many projections could be used, but the projection shown (which involves simple scaling of the control action) maintains the direction of the control action, which can be important for multivariable systems [2].

Now consider satisfying the first constraint (39) for general n. This is done by scaling the control action $\mathbf{u}$ calculated from the unconstrained control law (38):

$$\mathbf{u}^*(t) = \begin{cases} \mathbf{u}(t) & \max_i |\delta u_i(t)| \leq |\delta u|_{max} \\ \frac{|\delta u|_{max}}{\max_i |\delta u_i(t)|}\mathbf{u}(t) & \max_i |\delta u_i(t)| > |\delta u|_{max}. \end{cases} \tag{46}$$

In addition, the control action from the above equation is scaled to satisfy the second constraint (40):

$$\mathbf{u}^{\dagger}(t) = \begin{cases} \mathbf{u}^{*}(t) & \max_i |\delta^2 u_i^*(t)| \le |\delta^2 u|_{max} \\ \frac{|\delta^2 u|_{max}}{\max_i |\delta^2 u_i^*(t)|}\mathbf{u}^{*}(t) & \max_i |\delta^2 u_i^*(t)| > |\delta^2 u|_{max}. \end{cases} \tag{47}$$

$\mathbf{u}^{\dagger}$ satisfies both constraints (39) and (40).

This constraint-handling method is easy to implement and performs exactly as the unconstrained algorithm when constraint handling is not needed, and performs well when constraint handling is needed. Based on these considerations, it is recommended that this method be used to constrain the control action. That this method is preferable over using additional terms in the objective function is elucidated through simulations for the Avery pilot plant in Section 6.3.1.

Constrained Control Algorithm In summary, the constrained control algorithm is:

- Calculate the estimated state through (27).
- Calculate the unconstrained control move through (38).
- Scale the unconstrained control move using (46) and (47) to give the constrained control move.

4.4 Implemented Algorithm

Decreasing the Memory Requirement Because the unconstrained control action is scaled in (46) and (47) and is implemented *manually*, the *implemented* gap widths for the previous step will be somewhat different then the gap widths calculated by the unconstrained control algorithm for the previous step. The estimator (27) in the control algorithm should use the implemented gap widths, so the implemented gap widths $\mathbf{u}(t-1)$ are measured at each step in addition to $\hat{\mathbf{x}}(t)$. Implementation of the constrained control algorithm (27,38,46,47) requires that two vectors be stored at each step: $\mathbf{u}(t-2)$ and $\mathbf{x}(t-1|t-1)$ are needed to calculate $\mathbf{x}(t|t)$ in (27) ($\Delta\mathbf{u}(t-1) = \mathbf{u}(t-1)-\mathbf{u}(t-2)$). By defining a new variable ξ, the equations describing the control algorithm can be rearranged so that only one vector needs to be stored at each step. More specifically, introduce the vector $\xi(t-1)$ defined by

$$\xi(t-1) = \mathbf{x}(t-1|t-1) - \mathbf{C}\mathbf{u}(t-2). \tag{48}$$

Substituting $\mathbf{x}(t-1|t-1)$ from (48) into (25) and (27) gives

$$\mathbf{x}(t|t-1) = \mathbf{C}\mathbf{u}(t-1) + \xi(t-1) \tag{49}$$

$$\mathbf{x}(t|t) = \mathbf{C}\mathbf{u}(t-1) + (1-\gamma)\xi(t-1) + \gamma\left[\hat{\mathbf{x}}(t) - \mathbf{C}\mathbf{u}(t-1)\right]. \tag{50}$$

Now write (48) for the next time step

$$\xi(t) = \mathbf{x}(t|t) - \mathbf{C}\mathbf{u}(t-1). \tag{51}$$

A recursive formula for $\xi(t)$ can be found by substituting (50) into (51):

$$\xi(t) = (1-\gamma)\xi(t-1) + \gamma\left[\hat{\mathbf{x}}(t) - \mathbf{C}\mathbf{u}(t-1)\right]. \tag{52}$$

Then by substituting $\mathbf{x}(t|t)$ from (51) into the equation for the control move (38) and rearranging gives the control move in term of $\xi(t)$:

$$\mathbf{u}(t) = -(\mathbf{C}^T\mathbf{C})^{-1}\mathbf{C}^T\xi(t). \tag{53}$$

Implementing (53) requires storage of only the one vector $\xi(t-1)$ because $\xi(t)$ is calculated from $\xi(t-1)$, $\hat{\mathbf{x}}(t)$, and $\mathbf{u}(t-1)$ in (52), and $\hat{\mathbf{x}}(t)$ and $\mathbf{u}(t-1)$ are measured.

The control algorithm is initialized by measuring the adhesive thicknesses $\hat{\mathbf{x}}(0)$. Our best estimate of the state for the first sampling instance $\mathbf{x}(0|0)$ is the measured value $\hat{\mathbf{x}}(0)$. The initial gap widths are $\mathbf{u}(-1)$; we see from (51) that

$$\xi(0) = \mathbf{x}(0|0) - \mathbf{C}\mathbf{u}(-1) = \hat{\mathbf{x}}(0) - \mathbf{C}\mathbf{u}(-1). \tag{54}$$

The first control move $\mathbf{u}(0)$ is found from (53).

From (51) we see that $\xi(t)$ can be interpreted as an estimate for the disturbance. For a steady-state disturbance where the controller is turned on at $t = 0$, the best estimate for the disturbance is $\hat{\mathbf{x}}(0) - \mathbf{C}\mathbf{u}(-1)$, which is $\xi(0)$. Over time, filtering will improve the disturbance estimate $\xi(t)$ through (52). Measurement noise prevents a perfectly accurate disturbance estimate.

Decreasing On-Line Computation To decrease on-line computation, the matrix $(\mathbf{C}^T\mathbf{C})^{-1}\mathbf{C}^T$ pre-multiplying $\xi(t)$ in (53) is computed off-line.

Computer Implementation A computer implementation of the constrained control algorithm (54,52,53,46,47) involves the following steps:

1. Measurements
   - Measure dimensional variables $\breve{\mathbf{x}}$, $\breve{\mathbf{u}}$.
   - Transform to dimensionless variables $\mathbf{x}$, $\mathbf{u}$ using (11):

     $$x_i = \frac{\breve{x}_i - \bar{x}}{\bar{x}} \qquad u_i = \frac{\breve{u}_i - \bar{u}}{\bar{u}}, \tag{55}$$

     and augment $\mathbf{x}$ with a zero (19).
2. Computations
   - Update the disturbance estimate ξ using (54) or (52):

     $$\xi(t) = \begin{cases} \hat{\mathbf{x}}(0) - \mathbf{C}\mathbf{u}(-1) & \text{if } t = 0 \\ (1-\gamma)\xi(t-1) + \gamma\left[\hat{\mathbf{x}}(t) - \mathbf{C}\mathbf{u}(t-1)\right] & \text{if } t > 0, \end{cases} \tag{56}$$

     where $\mathbf{u}(-1)$ are the initial gap widths.

- Compute the unconstrained control move $\mathbf{u}$ using equation (53):

$$\mathbf{u}(t) = -(\mathbf{C}^T\mathbf{C})^{-1}\mathbf{C}^T\xi(t). \tag{53}$$

- Compute the constrained control move $\mathbf{u}^\dagger$ using equations (46) and (47):

$$\mathbf{u}^*(t) = \begin{cases} \mathbf{u}(t) & \max_i |\delta u_i(t)| \le |\delta u|_{max} \\ \frac{|\delta u|_{max}}{\max_i |\delta u_i(t)|}\mathbf{u}(t) & \max_i |\delta u_i(t)| > |\delta u|_{max}. \end{cases} \tag{46}$$

$$\mathbf{u}^\dagger(t) = \begin{cases} \mathbf{u}^*(t) & \max_i |\delta^2 u_i^*(t)| \le |\delta^2 u|_{max} \\ \frac{|\delta^2 u|_{max}}{\max_i |\delta^2 u_i^*(t)|}\mathbf{u}^*(t) & \max_i |\delta^2 u_i^*(t)| > |\delta^2 u|_{max}. \end{cases} \tag{47}$$

- Transform dimensionless gap widths $\mathbf{u}^\dagger$ to dimensional gap widths $\breve{\mathbf{u}}$ using (11):

$$\breve{u}_i = \bar{u}^\dagger u_i^\dagger + \bar{u}^\dagger. \tag{57}$$

3. Implement $\breve{\mathbf{u}}$
4. Go To Measurements

5 Limits of Performance

We would like to know how well the controller can be expected to reject disturbances in adhesive thicknesses. This leads us to study the various factors that *limit* the achievable closed loop performance. Knowledge of how these limitations affect the performance can show us how to modify the plant to improve the uniformity of the coating process. Also, because identification of model parameters is time-consuming and costly, we study how accurate the identification must be to achieve a given level of performance. We would also like to compare the performance of our control algorithm to the best closed-loop performance achievable by any control algorithm. This allows us to convince ourselves that we have indeed designed the best possible controller.

We begin by making the assumptions necessary to achieve perfect one-step rejection of disturbances. This provides a standard to which the various limitations on the closed loop performance can be compared.

Perfect Control We are interested in the ability of the controller to reject slow disturbances. Let us study the rejection of a steady-state disturbance and let the control algorithm start at $t = 0$. For simplicity of presentation, let the disturbance $\mathbf{d}$ have zero-mean and the initial gap widths $\mathbf{u}(-1) = \mathbf{0}$. We then make three assumptions:

1. no actuator constraints,
2. no measurement noise, and
3. our model is exactly equal to our plant.

Assumption 2 implies that the measured adhesive thicknesses at $t = 0$ is $\hat{\mathbf{x}}(0) = \mathbf{x}(0) = \mathbf{d}$. From the computation step (56) of the computer algorithm in Section 4.4 we have $\xi(0) = \mathbf{d}$. The control move for the first step from (53) is

$$\mathbf{u}(0) = -(\mathbf{C}^T\mathbf{C})^{-1}\mathbf{C}^T\mathbf{d}. \tag{58}$$

Assumption 1 implies that the unconstrained control move is equal to the constrained control move. If the operator implements the control move $\mathbf{u}(0)$ exactly, then applying assumption 2 to the plant (19) gives

$$\mathbf{x}(1) = \mathbf{C}\mathbf{u}(0) + \mathbf{d}. \tag{59}$$

Substituting $\mathbf{u}(0)$ from (58) into the above equation and grouping terms gives the adhesive thicknesses for the next time step

$$\mathbf{x}(1) = \left(\mathbf{I} - \mathbf{C}(\mathbf{C}^T\mathbf{C})^{-1}\mathbf{C}^T\right)\mathbf{d} \tag{60}$$

It can be shown that

$$\mathbf{I} - \mathbf{C}(\mathbf{C}^T\mathbf{C})^{-1}\mathbf{C}^T = \underbrace{\begin{pmatrix} \frac{1}{n} & \cdots & \frac{1}{n} & 0 \\ \vdots & \ddots & \vdots & \vdots \\ \frac{1}{n} & \cdots & \frac{1}{n} & 0 \\ 0 & \cdots & 0 & 0 \end{pmatrix}}_{(n+1)\times(n+1)}. \tag{61}$$

Substitute this into (60) and apply the assumption that the mean of the disturbance is zero to give

$$\mathbf{x}(1) = \begin{pmatrix} \frac{1}{n} & \cdots & \frac{1}{n} & 0 \\ \vdots & \ddots & \vdots & \vdots \\ \frac{1}{n} & \cdots & \frac{1}{n} & 0 \\ 0 & \cdots & 0 & 0 \end{pmatrix}\mathbf{d} = \begin{pmatrix} \frac{1}{n}\sum_{i=1}^{n} d_i \\ \vdots \\ \frac{1}{n}\sum_{i=1}^{n} d_i \\ 0 \end{pmatrix} = \begin{bmatrix} 0 \\ \vdots \\ 0 \\ 0 \end{bmatrix}. \tag{62}$$

We see that the controller under the assumptions perfectly rejects the steady-state disturbance in one step.

We will drop the assumptions of no actuator constraints, no measurement noise, and no model uncertainty in turn and show how each of these prevent the controller from rejecting the steady-state disturbance in one step. We will also investigate if the plant condition number limits performance.

5.1 Constraints on Actuator Movements

The constraints on the actuator positions will degrade performance only when the the control move from the unconstrained algorithm must be scaled to keep the gap widths feasible. It can be shown that in this case the adhesive thicknesses at the next time $\mathbf{x}(1)$ do not equal zero. We will also show below that the adhesive thicknesses $\mathbf{x}$ never reach zero.

Assume no measurement noise, that the model is perfect, and for simplicity of presentation that $\mathbf{d}$ has zero mean and the initial gap widths $\mathbf{u}(-1) = 0$. Then the measured adhesive thicknesses at $t = 0$ is $\hat{\mathbf{x}}(0) = \mathbf{x}(0) = \mathbf{d}$. From (56) we have $\xi(0) = \mathbf{d}$. The control move for the first step from (53) is

$$\mathbf{u}(0) = -(\mathbf{C}^T\mathbf{C})^{-1}\mathbf{C}^T\mathbf{d}. \tag{63}$$

If the control move from the unconstrained algorithm must be scaled to keep the gap widths feasible, the constrained control move is

$$\mathbf{u}^{\dagger}(0) = -\lambda(\mathbf{C}^T\mathbf{C})^{-1}\mathbf{C}^T\mathbf{d}, \tag{64}$$

where $0 < \lambda < 1$. If the operator implements the control move $\mathbf{u}^{\dagger}(0)$ exactly and there is no measurement noise, then applying the control move to the plant (19) gives

$$\mathbf{x}(1) = \mathbf{C}\mathbf{u}^{\dagger}(0) + \mathbf{d}. \tag{65}$$

Substituting $\mathbf{u}^{\dagger}(0)$ from (64) into the above equation and rearranging gives the adhesive thicknesses for the next time step

$$\mathbf{x}(1) = \left(\mathbf{I} - \lambda\mathbf{C}(\mathbf{C}^T\mathbf{C})^{-1}\mathbf{C}^T\right)\mathbf{d} \tag{66}$$

Similarly to (61), the above equation simplifies to

$$\mathbf{x}(1) = (1-\lambda)\mathbf{d}. \tag{67}$$

We see that the effect of the disturbance has been diminished by a factor of $1 - \lambda$.

Substituting $\xi(0)$, $\mathbf{x}(1)$, and $\mathbf{u}(0)$ from above into (56) and applying (61) gives the disturbance estimate

$$\xi(1) = \mathbf{d}. \tag{68}$$

We see that $\xi(1) = \xi(0)$. Under the assumptions, this implies that

$$\begin{array}{ll} \mathbf{u}(t) = \mathbf{u}(0) = -(\mathbf{C}^T\mathbf{C})^{-1}\mathbf{C}^T\mathbf{d} & \text{if } t \geq 0, \\ \mathbf{u}^{\dagger}(t) = \mathbf{u}^{\dagger}(0) = -\lambda(\mathbf{C}^T\mathbf{C})^{-1}\mathbf{C}^T\mathbf{d} & \text{if } t \geq 0, \\ \mathbf{x}(t) = \mathbf{x}(1) = (1-\lambda)\mathbf{d} & \text{if } t \geq 1, \quad \text{and} \\ \xi(t) = \xi(0) = \mathbf{d} & \text{if } t \geq 0. \end{array} \tag{69}$$

The constraints in gap widths prevent the steady-state disturbance from being completely rejected. This is true regardless of the control algorithm used.

Plant Modifications to Improve Performance The gap widths are constrained to prevent high stresses in the die. A die can be designed to have weaker constraints on its die gap widths by either placing the bolts further apart, by making the die lip thinner, or by making the die out of a more flexible metal. Putting the die bolts too far apart leads to strips of uncontrolled adhesive thickness between the die bolts. Making the die lip too thin can lead to a die lip that breaks easily. Making the die metal too flexible makes machining the die to tight tolerances difficult.

5.2 Measurement Noise

Measurement noise always limits performance.

Assume no actuator constraints, that the model is perfect, and for simplicity of presentation that $\mathbf{d}$ has zero mean and the initial gap widths $\mathrm{u}(-1) = 0$. Then from (19) the measured adhesive

thicknesses at $t = 0$ is $\hat{\mathbf{x}}(0) = \mathbf{x}(0) = \mathbf{d} + \mathbf{n}(0)$. From (56) we have $\xi(0) = \mathbf{d} + \mathbf{n}(0)$. The control move for the first step from (53) is

$$\mathbf{u}(0) = -(\mathbf{C}^T\mathbf{C})^{-1}\mathbf{C}^T(\mathbf{d} + \mathbf{n}(0)). \tag{70}$$

With no actuator constraints, $\mathbf{u}(0)$ above is also the constrained move. If the operator implements the control move exactly and there is no model uncertainty, then applying the control move to the plant (19) gives

$$\mathbf{x}(1) = \mathbf{C}\mathbf{u}(0) + \mathbf{d} + \mathbf{n}(1). \tag{71}$$

Substituting $\mathbf{u}(0)$ from (70) into the above equation, using (61), and rearranging gives the adhesive thicknesses for the next time step

$$\mathbf{x}(1) = \mathbf{n}(1) - \mathbf{C}(\mathbf{C}^T\mathbf{C})^{-1}\mathbf{C}^T\mathbf{n}(0). \tag{72}$$

This is nonzero for almost all values of measurement noise.

We see that the controller cannot drive the disturbance to zero in one step through a perfectly inverting controller. Noise corrupts the disturbance estimate $\xi(0)$, so the perfectly inverting controller also inverts the measurement noise, leading to an imperfect control move (compare (70) with (58)). This imperfect control move does not completely reject the disturbance (see (72)).

Noise filtering diminishes the effects of noise. To see this, substitute $\xi(0)$, $\mathbf{x}(1)$, and $\mathbf{u}(0)$ from above into (56) and apply (61) to give the disturbance estimate for the next time

$$\xi(1) = \mathbf{d} + (1 - \gamma)\mathbf{n}(0) + \gamma\mathbf{n}(1). \tag{73}$$

For $\gamma = 1$, the disturbance estimate $\xi(1) = \xi(0) = \mathbf{d} + \mathbf{n}(1)$, and there is no noise filtering. The controller cannot differentiate between the steady state disturbance and the random noise and is unable to accurately estimate the steady state disturbance, and therefore cannot reject it as effectively. When the filtering is increased ($\gamma \to 0$), the controller is able to obtain a better estimate of the steady state disturbance and is therefore more effective in eliminating it.

Increased noise filtering also slows the controller response time, so there is a tradeoff between improved coating uniformity and slower response times. We now define a measure for the uniformity of the coating and study this tradeoff in more detail.

Consider the closed loop system without disturbances, only measurement noise. For a stabilizing controller, the expected value for the estimated state $x(t|t)$ is zero. The estimated state will not exactly equal zero because the controller will treat the measurement noise as a disturbance and will try to reject it. Thus the estimated state will have some variance depending on the size of the noise. The variance of the estimated state $x(t|t)$ is an appropriate measure of the uniformity of the coating. For simplicity of presentation, assume a perfect model and that the noise at each gap position is equal—dropping these assumptions only slightly affects the following. Then it can be shown that

$$\text{Variance}(x_i) = \frac{\gamma}{2 - \gamma}\text{Variance}(n_i) \qquad \text{for } i = 1, \ldots, n. \tag{74}$$

An appropriate measure of the controller response time is the filter time constant plus 1 for the delay through the plant, *i.e.* $\tau + 1$.

Both Variance(x_i) and τ (though (29)) are functions of the noise filter parameter γ. Fig. 3 compares the controller response time versus the ratio of the variance of the state estimate to the

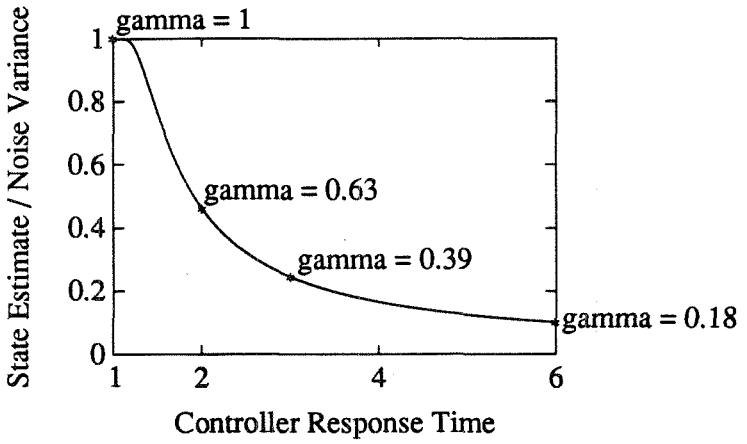

Figure 3: Comparison of variance of state estimate to measurement noise ratio versus controller response time.

measurement noise for different values of γ. A small amount of filtering ($\gamma \to 1$) corresponds to fast response times, but poor coating uniformity. A large amount of filtering corresponds to good coating uniformity, but with slow response times.

Plant Modifications to Improve Performance Ways to decrease the sensor noise should be investigated. To make sure the sensor noise is as small as possible, make sure that cables to the sensor are shielded adequately. Consider decreasing the distance between the sensor and the adhesive-coated paper to diminish the effect of air currents. Consider ways to decrease the vibration of the paper and the sensor. Of course an accurate sensor reading requires a stable film.

5.3 Model Uncertainty

Model uncertainty is the difference between the model and the plant. The error between the true behavior of the physical process and that predicted by the model can significantly affect the ability of the control system to perform adequately. Controllers that are insensitive to model uncertainty are said to be *robust.*

Let the plant gain matrix be $\mathbf{C_r}$, and assume no actuator constraints, no measurement noise, and for simplicity of presentation that $\mathbf{d}$ has zero mean and the initial gap widths $\mathbf{u}(-1) = 0$. Application of the control move (58) to the plant gives

$$\mathbf{x}(1) = \left(\mathbf{I} - \mathbf{C_r}(\mathbf{C}^T\mathbf{C})^{-1}\mathbf{C}^T\right)\mathbf{d}. \tag{75}$$

It can be shown that the adhesive thicknesses at the next time $\mathbf{x}(1)$ do not equal zero. Recall that part of the purpose of the correction equation (26) is to compensate for model uncertainty—as long as the closed loop system is stable, the disturbance *is* rejected, but only after several control moves.

Just how much uncertainty can affect the performance is not clear from (75). Below we quantify the effect of uncertainty. More specifically, we show that the control algorithm proposed in this paper is robust to gain uncertainty. Also, we will analyze the robustness as a function of the filter parameter γ to determine the effect of the noise filter on robustness.

Uncertainty in Gain Matrix The closed loop stability can be analyzed from the state-space equation for the closed loop system. A system will be considered stable when the effect of small disturbances remains small. A system is considered unstable when the effect of small disturbances grows until the constraints (39) and (40) are reached. The effect of disturbances will never grow unbounded because the constraints (39), (40), and $\sum_{i=1}^{n} u_i = 0$ hold, which bounds the magnitude of the control action.

Let the measurement be described in terms of the real plant:

$$\hat{\mathbf{x}}(t) = \mathbf{C_r}\mathbf{u}(t-1) + \mathbf{v_r}(t). \tag{76}$$

No assumptions are made on the unmeasured inputs $\mathbf{v_r}$.

Define $\mathbf{\Gamma}$ by

$$\mathbf{\Gamma} = -(\mathbf{C}^T\mathbf{C})^{-1}\mathbf{C}^T. \tag{77}$$

Then the control law (38) is given by

$$\mathbf{u}(t) = \mathbf{u}(t-1) + \mathbf{\Gamma}\mathbf{x}(t|t). \tag{78}$$

Substitute the model prediction of the previous time step $\mathbf{x}(t|t-1)$ from equation (25) and the measurement given by (76) into (26) to give the following equation when $t > 0$:

$$\mathbf{x}(t|t) = (1-\gamma)\mathbf{x}(t-1|t-1) + [\gamma\mathbf{C_r} + (1-\gamma)\mathbf{C}]\mathbf{u}(t-1) - (1-\gamma)\mathbf{C}\mathbf{u}(t-2) + \gamma\mathbf{v_r}(t). \tag{79}$$

Write (78) for step $t-1$ and rearrange:

$$\mathbf{u}(t-2) = \mathbf{u}(t-1) - \mathbf{\Gamma}\mathbf{x}(t-1|t-1). \tag{80}$$

Now substitute $\mathbf{u}(t-2)$ from (80) into (79) to give

$$\mathbf{x}(t|t) = (1-\gamma)(\mathbf{I}+\mathbf{C}\mathbf{\Gamma})\mathbf{x}(t-1|t-1) + \gamma\mathbf{C_r}\mathbf{u}(t-1) + \gamma\mathbf{v_r}(t). \tag{81}$$

Substitute $\mathbf{x}(t|t)$ from (81) into (78) to give

$$\mathbf{u}(t) = (1-\gamma)\mathbf{\Gamma}(\mathbf{I}+\mathbf{C}\mathbf{\Gamma})\mathbf{x}(t-1|t-1) + (\mathbf{I}+\gamma\mathbf{\Gamma}\mathbf{C_r})\mathbf{u}(t-1) + \gamma\mathbf{\Gamma}\mathbf{v_r}(t). \tag{82}$$

Let $\mathbf{u}(t)$ be a state, then (81) and (82) give the state-space equation that defines the closed loop system,

$$\begin{bmatrix} \mathbf{x}(t|t) \\ \mathbf{u}(t) \end{bmatrix} = \begin{bmatrix} (1-\gamma)(\mathbf{I}+\mathbf{C}\mathbf{\Gamma}) & \gamma\mathbf{C_r} \\ (1-\gamma)\mathbf{\Gamma}(\mathbf{I}+\mathbf{C}\mathbf{\Gamma}) & \mathbf{I}+\gamma\mathbf{\Gamma}\mathbf{C_r} \end{bmatrix} \begin{bmatrix} \mathbf{x}(t-1|t-1) \\ \mathbf{u}(t-1) \end{bmatrix} + \begin{bmatrix} \gamma \\ \gamma\mathbf{\Gamma} \end{bmatrix} \mathbf{v_r}(t), \tag{83}$$

with initial conditions

$$\begin{bmatrix} \mathbf{x}(0|0) \\ \mathbf{u}(0) \end{bmatrix} = \begin{bmatrix} \hat{\mathbf{x}}(0) \\ \mathbf{u}(-1) - \mathbf{\Gamma}\hat{\mathbf{x}}(0) \end{bmatrix}. \tag{84}$$

For a discrete time system, we have closed loop stability if and only if the eigenvalues of

$$\mathbf{A} = \begin{bmatrix} (1-\gamma)(\mathbf{I}+\mathbf{C}\mathbf{\Gamma}) & \gamma\mathbf{C_r} \\ (1-\gamma)\mathbf{\Gamma}(\mathbf{I}+\mathbf{C}\mathbf{\Gamma}) & \mathbf{I}+\gamma\mathbf{\Gamma}\mathbf{C_r} \end{bmatrix} \tag{85}$$

are inside the unit circle. More specifically, the effect of disturbances will decay to zero if the spectral radius of $\mathbf{A}$ is less than one, and the effect of small disturbances will grow until the constraints are met when the spectral radius of $\mathbf{A}$ is greater than one [1].

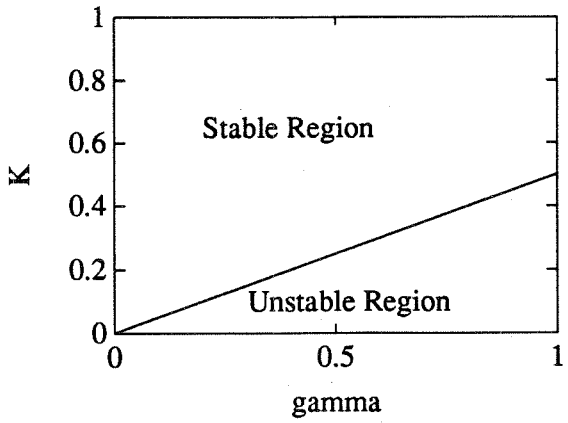

Figure 4: Closed loop stability as a function of γ and $K = \frac{k}{k_r}$, no interaction uncertainty.

Uncertainty in Gain This section considers uncertainty in the gain; interaction uncertainty for the Avery pilot plant will be considered in Section 6.3.2. The real gain will be denoted as k_r and the augmented real plant is

$$\mathbf{C_r} = \begin{bmatrix} k_r\mathbf{B} \\ 1 \cdots 1 \end{bmatrix}. \tag{86}$$

Recall that k is the gain and $\mathbf{C}$ is the gain matrix for the model.

By calculating the eigenvalues of $\mathbf{A}$ in (85) we determine which values of the ratio $K = \frac{k}{k_r}$ give a stable closed loop system. Fig. 4 shows which values of K give a stable closed loop system for each value of filter parameter γ. If the gain of the real plant is not underestimated by more than a factor of two ($K > \frac{1}{2}$), then the closed loop system is stable. For increased filtering (smaller γ), the model gain k need not be as accurate. In other words, increased filtering adds robustness to gain uncertainty.

The plant gain need not be known accurately for the controller to remain stable. Uncertainty in the plant gain will lead only to slower rejection of disturbances. Since we need approximate only the plant gain to design the controller, detailed identification runs are not needed to design the controller! Any reasonable estimate will do. This makes it easier to apply the control algorithm to new cross-directional systems when $\breve{k}$ does not change much between systems.

It can be shown that the stability boundary in Fig. 4 is the straight line given by $k = \frac{1}{2}\gamma k_r$.

5.4 The Plant Condition Number

It is well-known that high condition number plants (called *ill-conditioned*) can be difficult to control [5, 7, 8]. By the condition number we mean

$$\kappa(\mathbf{C}) \equiv \frac{\overline{\sigma}(\mathbf{C})}{\underline{\sigma}(\mathbf{C})}, \tag{87}$$

where $\overline{\sigma}$ and $\underline{\sigma}$ denote the maximum and minimum singular values of the plant

$$\overline{\sigma}(\mathbf{C}) = \max_{\mathbf{u}\neq 0} \frac{\|\mathbf{Cu}\|_2}{\|\mathbf{u}\|_2}, \qquad \underline{\sigma}(\mathbf{C}) = \min_{\mathbf{u}\neq 0} \frac{\|\mathbf{Cu}\|_2}{\|\mathbf{u}\|_2}. \tag{88}$$

A plant with a high condition number is characterized by strong directionality because inputs in directions corresponding to high plant gains are strongly amplified by the plant, while inputs in directions corresponding to low plant gains are not. Thus ill-conditioned plants may be sensitive to actuator uncertainty ([8]).

Recall from Section 2.4 that $\mathbf{C} = \begin{bmatrix} k\mathbf{B} \\ 1 \cdots 1 \end{bmatrix}$. The last row of $\mathbf{C}$ was augmented to the plant matrix $k\mathbf{B}$ to keep $\mathbf{u}$ from straying from zero. The elements of the last row of $\mathbf{C}$ need not be 1's—the last row can be any constant multiplied by a row of 1's. The controllability of the process is not dependent on what scalar is used in the last row of $\mathbf{C}$, so a true measure of the controllability of the process must be independent of this scalar. A "true" measure of the controllability of the plant can be defined as

$$\kappa^*(\mathbf{C}) \equiv \inf_s \kappa \left(\begin{bmatrix} k\mathbf{B} \\ s \cdots s \end{bmatrix} \right). \tag{89}$$

κ^* was calculated for plants with different numbers of actuators n. For all n, κ^* was 1. This means that ill-conditioning is not a serious problem for cross-directional processes of the type studied here.

6 Application to Avery Label-Producing Pilot Plant

The theory developed in the preceding section is applied to the control of a label-producing pilot plant at Avery Research Company (see Fig. 1).

First the model is identified and the model assumptions are justified based on input-output data. Then simulations and models for the noise and the disturbance are used to tune the noise filter. The limitations on the closed loop performance are then investigated, with respect to constraints, noise, and interaction uncertainty. We conclude the section with experimental closed loop testing of the controller.

6.1 Identification and Justification of Model Assumptions

For the pilot plant, the nominal gap width $\bar{u} = 20$ mils and the number of actuators $n = 12$. We identify from input-output data models for the disturbance, noise, and gain matrix $\mathbf{P}$. The input-output data are also used to justify the assumptions used to develop the models.

Disturbance The plant gain k was fitted as discussed in Section 2.3.2 to give $k = 0.17$. The residuals $\mathbf{z}$ were biased (see Fig. 5). This suggests that $\mathbf{v}$ should be separated into two parts, $\mathbf{v} = \mathbf{d} + \mathbf{n}$, where $\mathbf{d}$ accounts for the bias, and $\mathbf{n}$ accounts for the random nature of $\mathbf{v}$. So the model for each experiment from (14) is

$$\mathbf{x}^i = k\mathbf{B}\mathbf{u}^i + \mathbf{d} + \mathbf{n}^i \qquad i = 1, \ldots, m. \tag{90}$$

We fit k and $\mathbf{d}$ from the input-output data by least squares similarly as in Section 2.3.2. To do

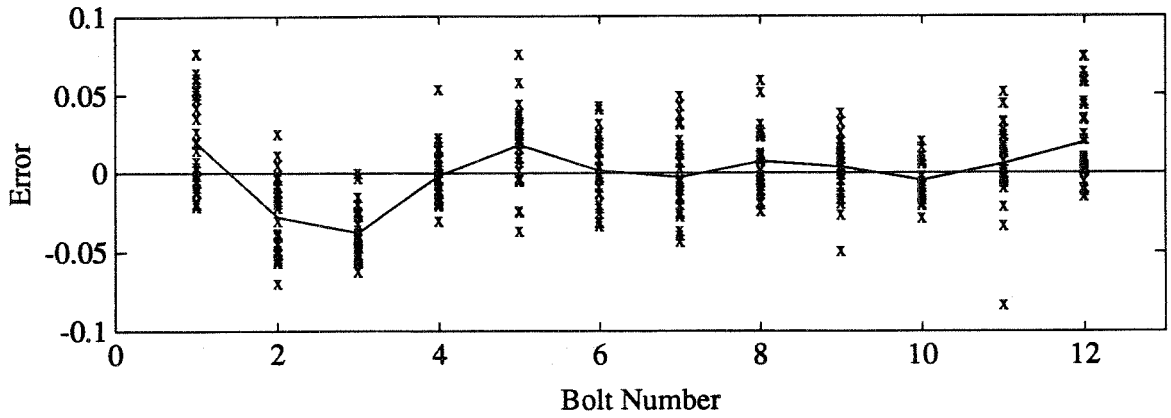

Figure 5: Residuals from fitting the plant gain k without a disturbance term $\mathbf{d}$.

this, stack equations (90) on top of each other and rearrange to give

$$\begin{pmatrix} \mathbf{x}^1 \\ \vdots \\ \mathbf{x}^m \end{pmatrix} = \begin{pmatrix} \mathbf{B}\mathbf{u}^1 & \mathbf{I} \\ \vdots & \vdots \\ \mathbf{B}\mathbf{u}^m & \mathbf{I} \end{pmatrix} \begin{pmatrix} k \\ \mathbf{d} \end{pmatrix} + \begin{pmatrix} \mathbf{n}^1 \\ \vdots \\ \mathbf{n}^m \end{pmatrix}. \tag{91}$$

Define

$$\mathbf{A} = \begin{pmatrix} \mathbf{B}\mathbf{u}^1 & \mathbf{I}_n \\ \vdots & \vdots \\ \mathbf{B}\mathbf{u}^m & \mathbf{I}_n \end{pmatrix}, \quad \mathbf{b} = \begin{pmatrix} \mathbf{x}^1 \\ \vdots \\ \mathbf{x}^m \end{pmatrix}, \quad \mathbf{y} = \begin{pmatrix} k \\ \mathbf{d} \end{pmatrix}, \quad \text{and} \quad \mathbf{z} = -\begin{pmatrix} \mathbf{n}^1 \\ \vdots \\ \mathbf{n}^m \end{pmatrix}. \tag{92}$$

We are interested in fitting the dimensionless plant gain k and the steady state disturbance $\mathbf{d}$. We assume that the measurement noise $\mathbf{n}^i$ are independent of the inputs $\mathbf{u}^i$. Then a natural objective for selecting $\begin{pmatrix} k \\ \mathbf{d} \end{pmatrix}$ is to minimize the square norm of the residual vector $\mathbf{z} = \mathbf{A}\mathbf{y} - \mathbf{b}$. This is the least squares problem

$$\min_{\mathbf{y}} (\mathbf{A}\mathbf{y} - \mathbf{b})^T (\mathbf{A}\mathbf{y} - \mathbf{b}). \tag{93}$$

The solution $\mathbf{y} = \begin{pmatrix} k \\ \mathbf{d} \end{pmatrix}$ that solves the least squares problem is given by

$$k = 0.18, \quad \mathbf{d} = \begin{bmatrix} 0.0187 \\ -0.0284 \\ -0.0381 \\ -0.0013 \\ 0.0182 \\ 0.0016 \\ -0.0027 \\ 0.0072 \\ 0.0041 \\ -0.0043 \\ 0.0056 \\ 0.0194 \end{bmatrix} \tag{94}$$

The input-output data were collected over two days. If the parameters are fit to the data from each day separately, Fig. 6 shows that the bias vector $\mathbf{d}$ retains much of its character between days. It

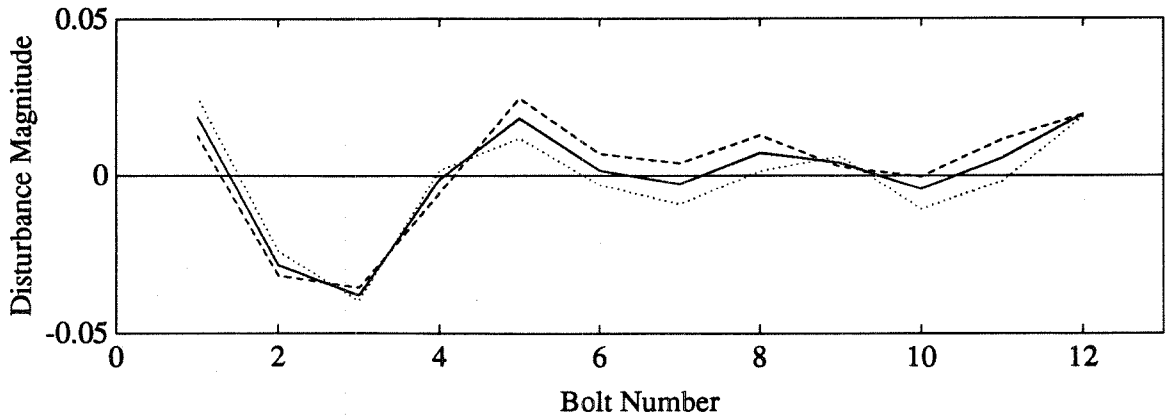

Figure 6: Bias vectors **d** for day 1 and day 2. The dotted line is day 1. The dashed line is day 2. The solid line is the average over both days.

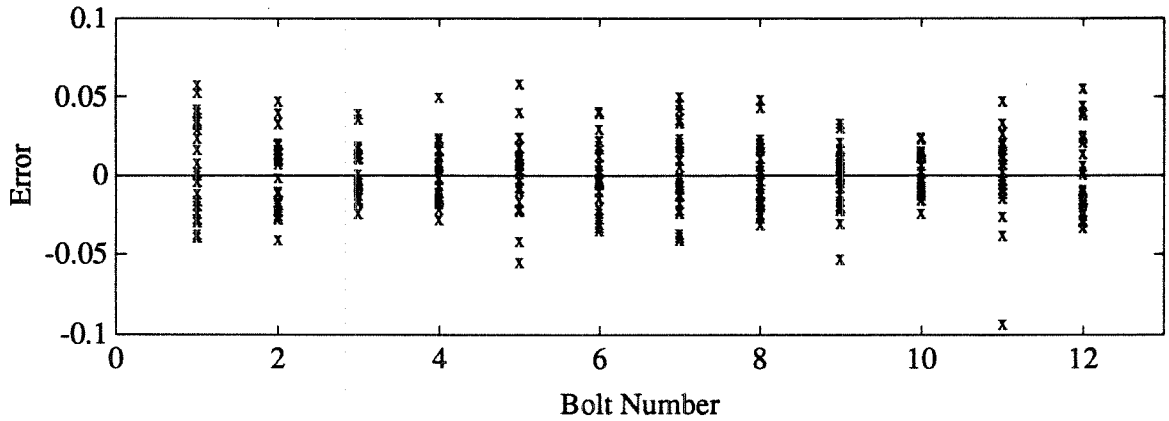

Figure 7: Residuals from fitting the plant gain k and a disturbance term **d**.

is therefore reasonable to assume that much of this bias is not *transient* but rather represents a basic characteristic of the physical system. Its origin could be due to several factors, for instance roller imperfections, inexact calibration of the gap widths, or different drying rates (recall that the coating thickness is measured after the adhesive is dried). This justifies the assumption that the bias **d** is steady state. We refer to **d** as the steady-state disturbance.

$\mathbf{n}^i = \mathbf{x}^i - k\mathbf{B}\mathbf{u}^i - \mathbf{d}$ is calculated for all the experiments and plotted in Fig. 7. We see that **n** is unbiased. We refer to **n** as the measurement noise.

Noise We determine a specific noise model to be used for simulations in Section 6.2.

Fig. 7 suggests that the measurement noise **n** would be described reasonably well by a normally-distributed stochastic variable, where each element of **n** is independent, and n_i is described as a normally-distributed random variable with zero mean and standard deviation σ, *i.e.* n_i has the

probability distribution function [4]

$$f(n_i) = \frac{1}{\sqrt{2\pi}\sigma} e^{-n_i^2/2\sigma^2}. \tag{95}$$

From Fig. 7 we see that it is reasonable to assume an equal standard deviation for each gap position. Then an unbiased estimate of the noise variance is [4]

$$\text{Variance}(n_i) = \sigma^2 = \frac{1}{mn-1} \sum_{i=1}^{mn} z_i^2 = 0.00046, \tag{96}$$

where $\mathbf{z} = \mathbf{A} \begin{pmatrix} k \\ \mathbf{d} \end{pmatrix} - \mathbf{b}$.

To doublecheck that we have a reasonable model for the measurement noise $\mathbf{n}$, adhesive thicknesses for consecutive measurements without changing the gap widths were measured and compared to the residuals in Fig. 7. They were found to agree.

Gain matrix P To test the assumptions used to develop the form of the gain matrix $\mathbf{P}$ in Section 2.1, we dropped all the assumptions and fitted the entire 12×12 gain matrix in (2) to the data for a total of 144 parameters—we denote this matrix by $\mathbf{P}_{144}$. This model gives little improvement over the gain matrix $\mathbf{P}$ resulting from the assumptions, so the assumptions are valid.

A very small interaction between nearest-neighbor positions was observed, so the assumption 3 in Section 2.1 would not have been justified if the spacing between actuators/sensors had been much smaller.

6.2 Tuning the Noise Filter

Discrete time process simulations were performed using the above control law. The ability of the controller to remove steady state disturbances was studied. For all simulations, the real system was assumed to be given by $\mathbf{P}_{144}$ above. Our model $\mathbf{P}$ assumes no interactions between the ith actuator and the jth sensor for $i \neq j$, except through the constant flow condition, and this assumption is not completely valid. Using $\mathbf{P}$ for the simulations would make the controller look better than it really is; $\mathbf{P}_{144}$ should give a better idea on how well the controller performs. In robust control language, we are accounting for *interaction uncertainty*. Explicit uncertainty in the interactions and in the plant gain k is explored in Section 6.3.2.

To study the effect of the noise filter parameter γ on the closed loop performance, γ was varied from 0.1 to 1. Ten controller moves were simulated using equation (38) and 2.6**d** as the steady state disturbance, where $\mathbf{d}$ is given in equation (94). This disturbance was chosen because its shape is known to be representative of disturbances encountered in the pilot plant and it was scaled so that its largest element corresponded to a 10% fluctuation in $\mathbf{x}$, which, according to Avery, is a typical magnitude for coating imperfections found in production.

Plots of the measured adhesive thicknesses $\hat{\mathbf{x}}(t)$, the control move $\mathbf{u}(t)$, and the estimated state $\mathbf{x}(t|t)$ are shown in Appendix I.

For $\gamma = 0.1$, the control algorithm acts too slowly to reject the disturbance within 10 time steps (the estimated state $\mathbf{x}(10|10)$ is nonzero). By comparing $\mathbf{u}(t)$ and $\mathbf{x}(t|t)$ for $\gamma = 0.1$ with $\mathbf{u}(t)$ and $\mathbf{x}(t|t)$ for larger γ, we see that for increasing γ the control algorithm moves faster to reject the disturbance.

For γ near 1, the lack of noise filtering prevents the control algorithm from accurately estimating the disturbance; this is seen by the erratic estimated state $\mathbf{x}(t|t)$. The erratic estimated state leads to erratic control moves, and the disturbance rejection is poor. For smaller γ, the controller rejects disturbances more thoroughly (for example, compare the estimated state at $t = 10$ for $\gamma = 0.4$ and $\gamma = 1$).

The "best" value for γ is determined by trading off the speed the disturbance is rejected with the final uniformity of the coating.

6.3 Limits of Performance

Below we consider the limitations on performance by the actuator constraints and interaction uncertainty. The effect of measurement noise on performance was discussed in the above section.

6.3.1 Handling Actuator Constraints

Two methods of handling actuator constraints are compared:

1. adding additional terms in the objective function (discussed in Section 4.3.1)
2. scaling control moves to the feasible region (discussed in Section 4.3.3)

The dimensionless actuator constraints for the pilot plant are approximated by

$$|\delta u_i| = |u_{i+1} - u_i| \leq 0.05, \qquad \text{for } i = 1, \ldots, n-1, \tag{97}$$

and

$$|\delta^2 u_i| = |u_{i+2} - 2u_{i+1} + u_i| \leq 0.10, \qquad \text{for } i = 1, \ldots, n-2. \tag{98}$$

The second group of constraints (98) implies the first group of constraints (97) and are not considered further.

Methods 1 and 2 are compared through closed loop simulations. We chose a steady state disturbance $\mathbf{d}_{\text{test}}$ large enough so that rejecting $\mathbf{d}_{\text{test}}$ would necessitate an infeasible controller output, but rejecting $\frac{2}{3}\mathbf{d}_{\text{test}}$ would not. $\gamma = 0.7$ was used for the simulations. Measurement noise was ignored to aid in comparing methods 1 and 2.

First, the unconstrained algorithm (38) was used with $\mathbf{d}_{\text{test}}$ and $\frac{2}{3}\mathbf{d}_{\text{test}}$. As shown in Fig. 8 both disturbances were rejected. The control move for Fig. 8a did not satisfy the actuator constraints whereas the control move for Fig. 8b did.

The controller output for method 1 (43) is constrained to be feasible by choosing β_1 large enough (let $\beta_2 = 0$). We chose β_1 just large enough so that the actuator constraints were satisfied for

$\mathbf{d} = \mathbf{d}_{\text{test}}$. From Fig. 9a we see that $\mathbf{d}_{\text{test}}$ is not rejected as required by the physical constraints on the system. Simulating the system with $\mathbf{d} = \frac{2}{3}\mathbf{d}_{\text{test}}$ gave Fig. 9b. We see that the implementation of the penalty $\beta_{1,\text{optimal}}$ also prevented the controller from rejecting $\frac{2}{3}\mathbf{d}_{\text{test}}$, though this disturbance can be rejected while satisfying the actuator constraints.

Now consider method 2. Again, $\mathbf{d}_{\text{test}}$ and $\frac{2}{3}\mathbf{d}_{\text{test}}$ were used as disturbances. The results are shown in Fig. 10. For $\mathbf{d} = \mathbf{d}_{\text{test}}$, the algorithm tries to reject the disturbance while keeping the actuator positions feasible, but it cannot. For the smaller disturbance, the actuator constraints are met while rejecting the disturbance in the same manner as the unconstrained algorithm.

To summarize:

- For method 1, to choose β_1 large enough to keep the actuator positions feasible for large disturbances prevents disturbance rejection for all disturbances.
- For method 2, large disturbances are rejected as much as possible while satisfying the actuator constraints while small disturbances are rejected completely. Method 2 not only eliminates the need of an additional tuning parameter making it simpler to implement, but also provides better performance over a wider range of disturbances and is therefore preferable to method 1.

6.3.2 Interaction Uncertainty

The effect of interaction uncertainty on the stability of the closed loop system was investigated using the model fit to the Avery plant data. This was done following the same procedure as in Section 5.3, but using $\mathbf{C_r} = \begin{pmatrix} \mathbf{P}_{144} \\ 1 \cdots 1 \end{pmatrix}$ for the real plant and $\mathbf{C} = \begin{pmatrix} k\mathbf{B} \\ 1 \cdots 1 \end{pmatrix}$ for the model. Fig. 11 shows the stable region as a function of the normalized model gain $K = \frac{k}{k_r}$ where k_r here denotes the best fit gain. As in Fig. 4, the boundary between the stable and unstable regions is a straight line, but the slope in Fig. 11 is steeper. Introducing interaction uncertainty decreases the stable region, but an accurate estimate of k is still not required.

6.4 Experimental Closed Loop Control

Experimental work was to be completed in August at Avery Research Center.

7 Conclusions

A model predictive control algorithm was presented which rejects slow disturbances in coating thicknesses. It was shown how to find the one parameter of the model, the model gain, off-line or from input-output data. The control algorithm has one tuning parameter γ, which trades robustness to model error and insensitivity to measurement noise with speed of response.

Several constraint-handling methods were compared. The simplest yet effective constraint-handling method involved scaling the control action by a scalar which was just large enough to make the

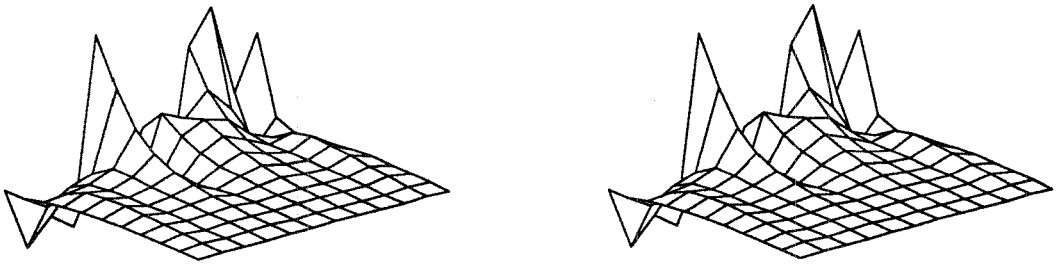

max |dl = 0.0525 max |dl = 0.0394

Figure 8: Unconstrained algorithm (38) on $\mathbf{d}_{\text{test}}$ and $\frac{2}{3}\mathbf{d}_{\text{test}}$.

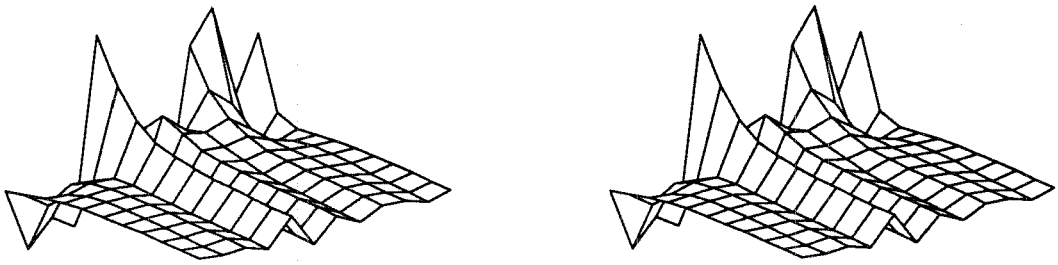

max |dl = 0.0525 max |dl = 0.0394

Figure 9: Effect of $\beta_1 = 0.21$, $\beta_2 = 0$ in equation (43) on $\mathbf{d}_{\text{test}}$ and $\frac{2}{3}\mathbf{d}_{\text{test}}$.

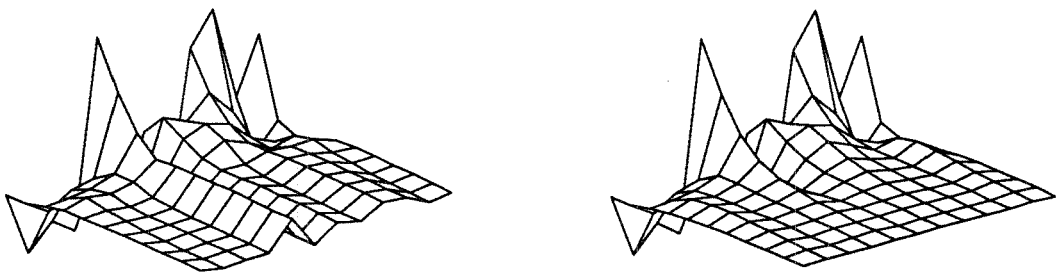

max |dl = 0.0525 max |dl = 0.0394

Figure 10: Constraining algorithm (38) with (46) on $\mathbf{d}_{\text{test}}$ and $\frac{2}{3}\mathbf{d}_{\text{test}}$.

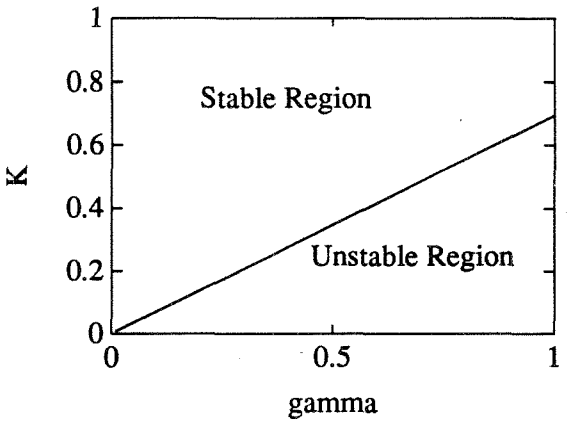

Figure 11: Closed loop stability as a function of γ and $K = \frac{k}{k_r}$. Interaction uncertainty was included through the use of $\mathbf{P_{144}}$.

control action feasible.

Actuator constraints, measurement noise, model uncertainty, and the plant condition number are investigated to determine which of these limit the achievable closed loop performance. Knowledge of how these limitations affect the performance suggested how to modify the plant to improve the uniformity of the coating process. Also we found that the controller was very forgiving of a poor gain estimate. This means that identification runs are not needed to design the controller when we have a reasonable estimate of the plant gain!

The theory developed throughout the paper was rigorously verified though simulations and experiments on a pilot plant adhesive coating process at Avery Research Co. in Pasadena. The effect of interactions on the closed loop performance was shown to be negligible *for this pilot plant.* The measurement noise and the actuator constraints were shown to have the largest effect on closed loop performance.

References

[1] K. J. Åström and B. Wittenmark. *Computer Controlled Systems Theory and Design.* Prentice-Hall, Inc., Englewood Cliffs,N.J., 1984.

[2] P. J. Campo. *Studies In Robust Control Of Systems Subject To Constraints.* PhD thesis, California Institute of Technology, Pasadena, 1990.

[3] J. H. Lee. *Robust Inferential Control: A Methodology for Control Structure Selection and Inferential Control System Design in the Presense of Model/Plant Mismatch.* PhD thesis, California Institute of Technology, Pasadena, 1991.

[4] L. Ljung. *System identification: theory for the user.* Prentice-Hall, Englewood Cliffs, New Jersey, 1987.

[5] M. Morari and J. C. Doyle. A unifying framework for control system design under uncertainty and its implications for chemical process control. In M. Morari and T. J. McAvoy, editors, *Third International Conference on Chemical Process Control (CPC III)*, Amsterdam, 1986. Elsevier.

[6] L. Sartor. *Slot Coating: Fluid Mechanics and Die Design.* PhD thesis, University of Minnesota, citynamehere, 1990.

[7] S. Skogestad and M. Morari. Design of resilent processing plants—ix. effect of model uncertainty on dynamic resilience. *Chemical Engineering Science*, 42(7):1765–1780, July 1987.

[8] S. Skogestad, M. Morari, and J. C. Doyle. Robust control of ill-conditioned plants: High purity distillation. *IEEE Transactions on Automatic Control*, AC-33:1092–1105, Dec. 1988.

Appendix I

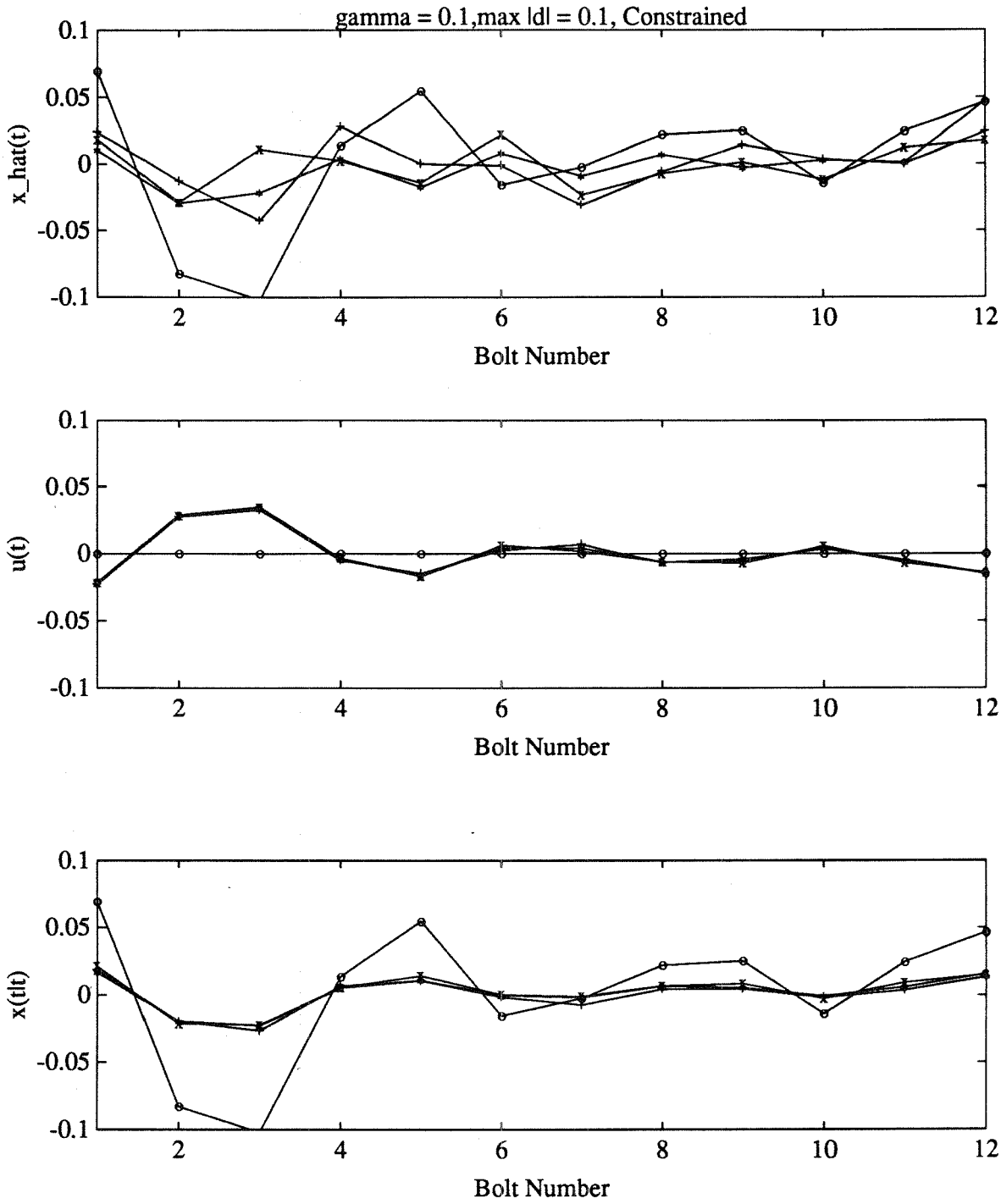

Figure 12: Profiles of the measured adhesive thicknesses $\hat{\mathbf{x}}(t)$, control moves $\mathbf{u}(t)$, and estimated states $\mathbf{x}(t|t)$ at times $t = 0$ (o), $t = 1$ (x), $t = 4$ (*), and $t = 10$ (+) for $\gamma = 0.1$.

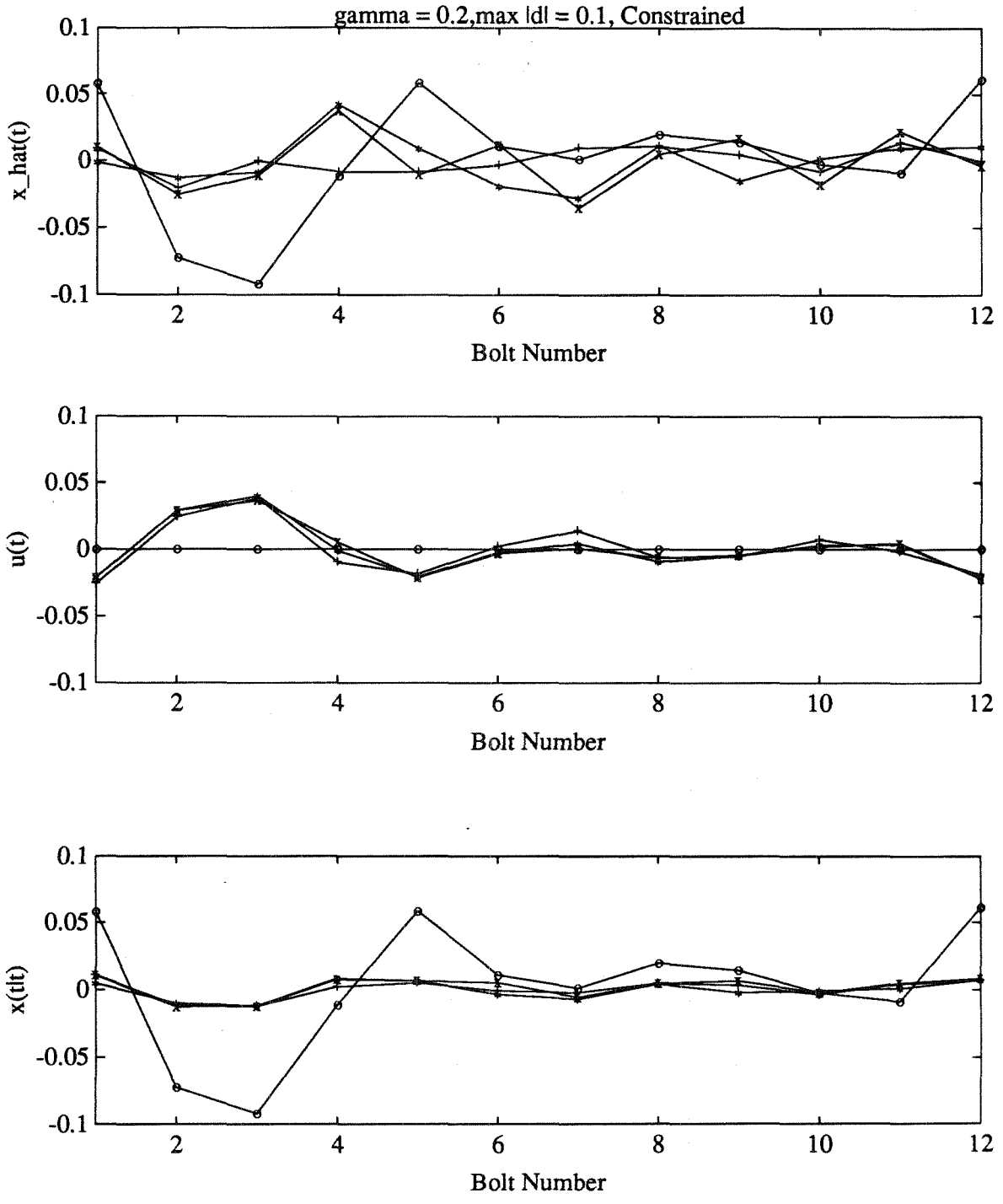

Figure 13: Profiles of the measured adhesive thicknesses $\hat{\mathbf{x}}(t)$, control moves $\mathbf{u}(t)$, and estimated states $\mathbf{x}(t|t)$ at times $t = 0$ (o), $t = 1$ (x), $t = 4$ (*), and $t = 10$ (+) for $\gamma = 0.2$.

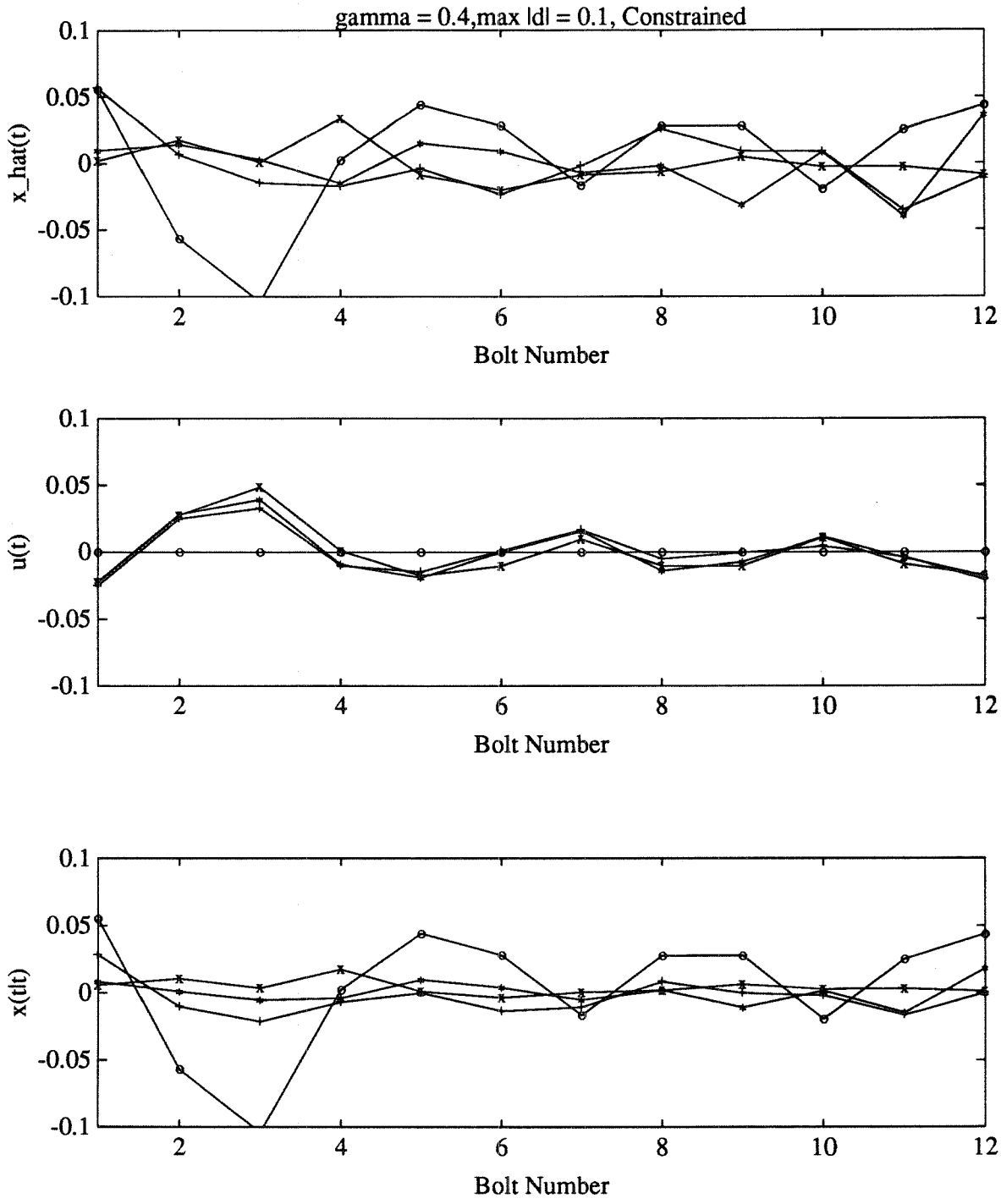

Figure 14: Profiles of the measured adhesive thicknesses $\hat{\mathbf{x}}(t)$, control moves $\mathbf{u}(t)$, and estimated states $\mathbf{x}(t|t)$ at times $t = 0$ (o), $t = 1$ (x), $t = 4$ (*), and $t = 10$ (+) for $\gamma = 0.4$.

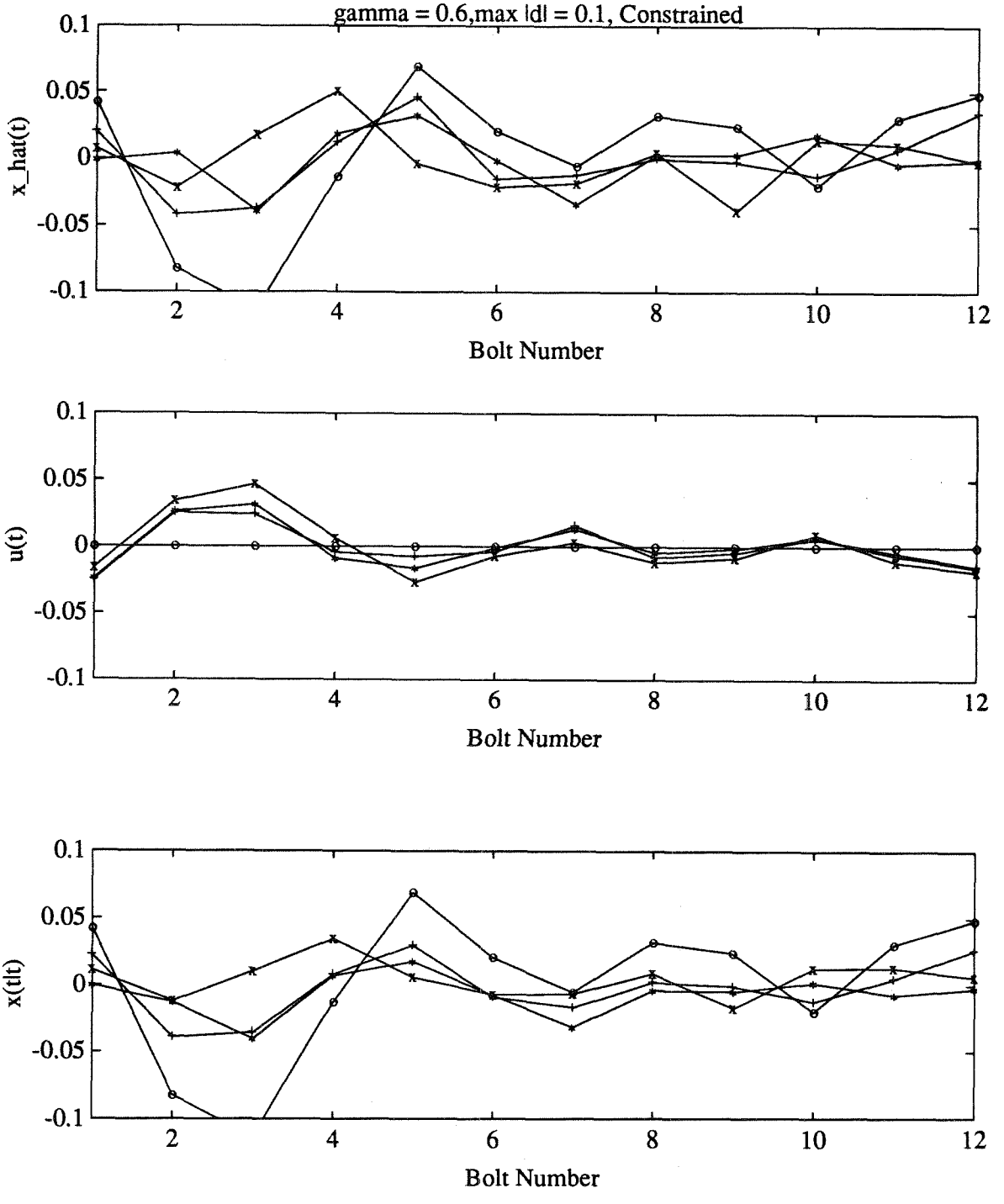

Figure 15: Profiles of the measured adhesive thicknesses $\hat{\mathbf{x}}(t)$, control moves $\mathbf{u}(t)$, and estimated states $\mathbf{x}(t|t)$ at times $t = 0$ (o), $t = 1$ (x), $t = 4$ (*), and $t = 10$ (+) for $\gamma = 0.6$.

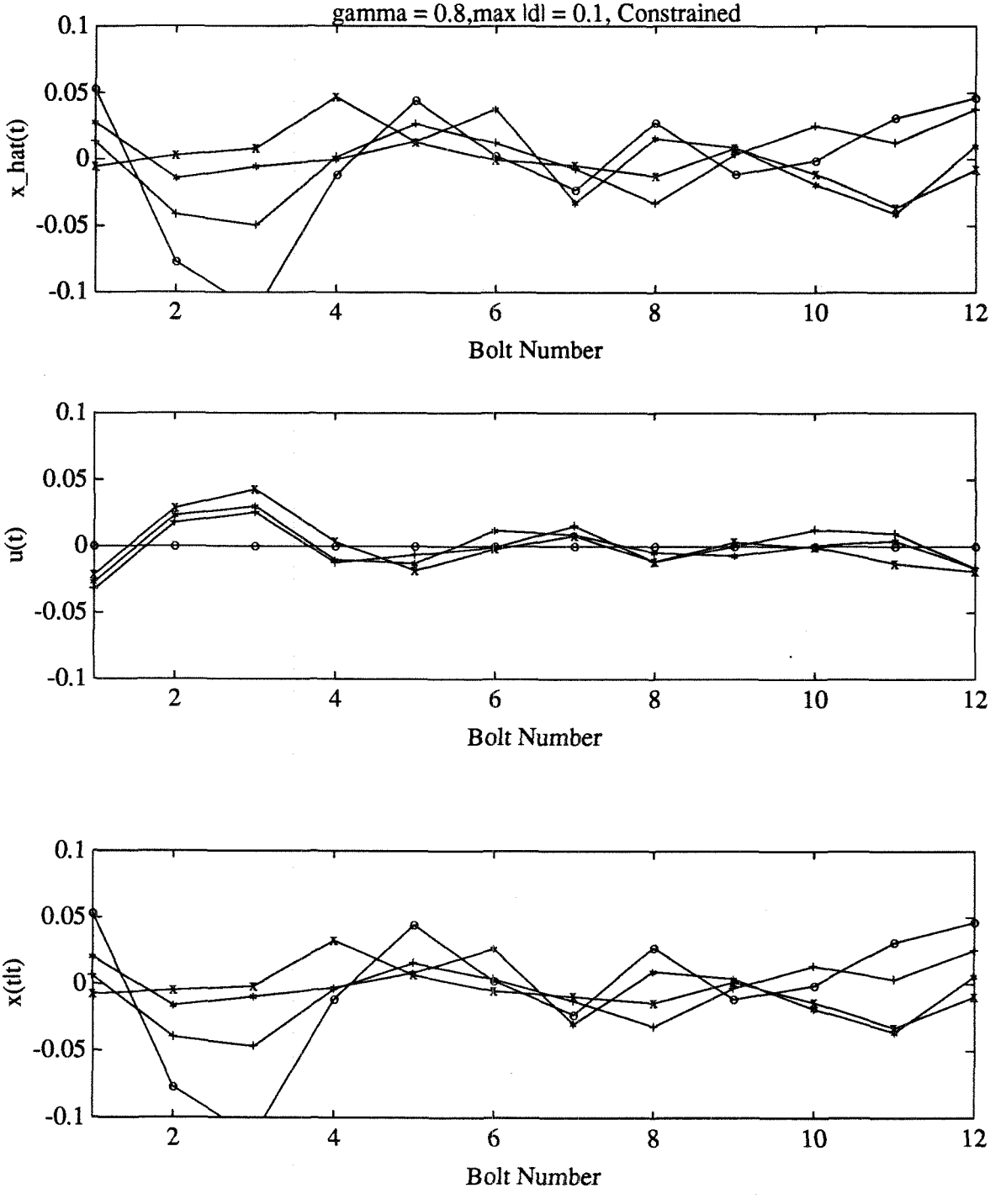

Figure 16: Profiles of the measured adhesive thicknesses $\hat{\mathbf{x}}(t)$, control moves $\mathbf{u}(t)$, and estimated states $\mathbf{x}(t|t)$ at times $t = 0$ (o), $t = 1$ (x), $t = 4$ (*), and $t = 10$ (+) for $\gamma = 0.8$.

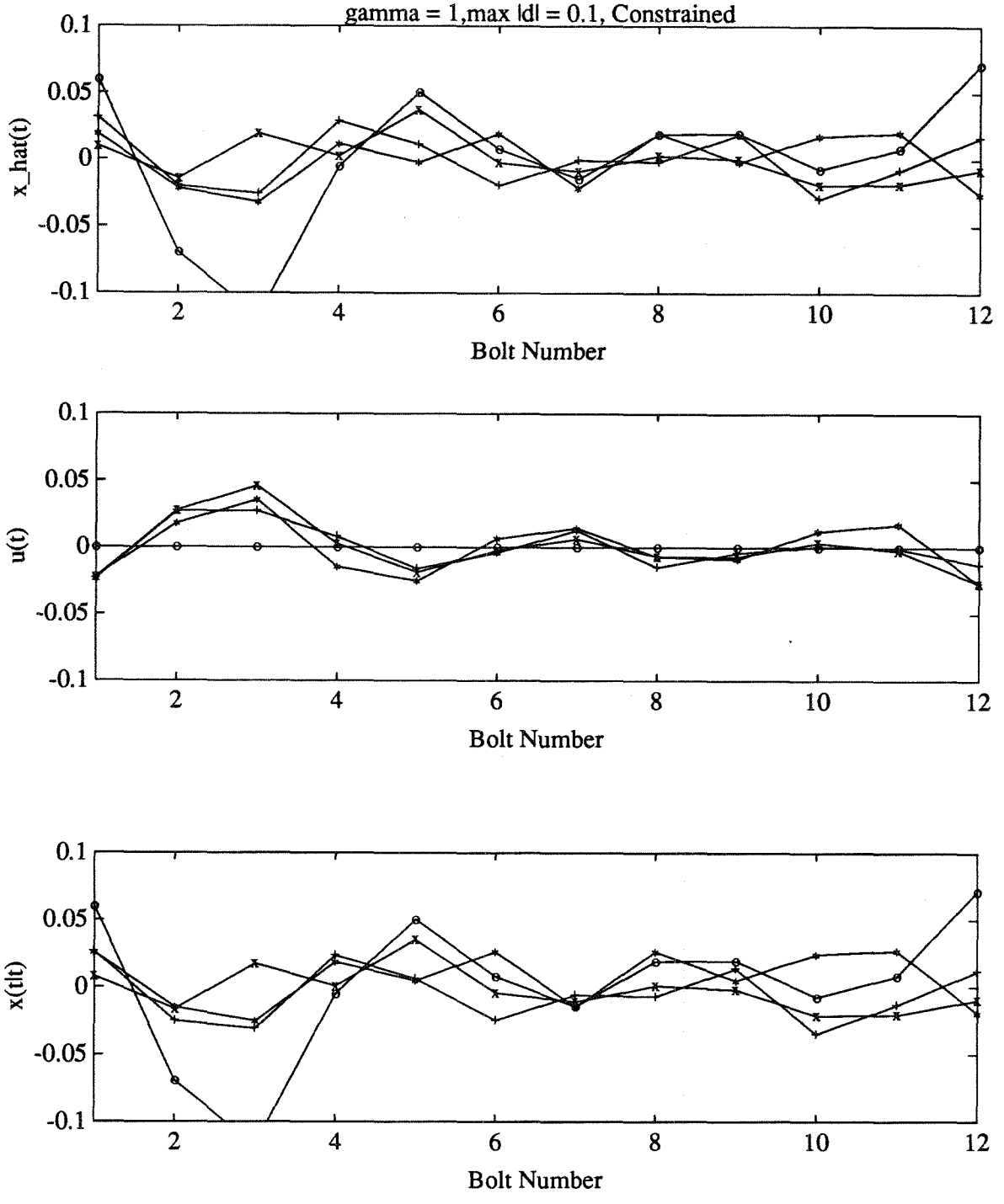

Figure 17: Profiles of the measured adhesive thicknesses $\hat{\mathbf{x}}(t)$, control moves $\mathbf{u}(t)$, and estimated states $\mathbf{x}(t|t)$ at times $t = 0$ (o), $t = 1$ (x), $t = 4$ (*), and $t = 10$ (+) for $\gamma = 1$.